Electronic Supplementary Material (ESI) for Environmental Science: Processes & Impacts.

Supporting Information

Surface-water/groundwater boundaries affect seasonal PFAS concentrations and PFAA precursor transformations

Environmental Science: Processes & Impacts

Andrea Kristina Tokranov,[ab] Denis R. LeBlanc,[b] Heidi M. Pickard,[a] Bridger J. Ruyle,[a] Larry B. Barber,[c] Robert B. Hull,[b] Elsie M. Sunderland[ad] and Chad David Vecitis[a]*

[a.] *Harvard John A. Paulson School of Engineering and Applied Sciences, Cambridge, MA 02138. E-mail: andrea_tokranov@alumni.harvard.edu*
[b.] *U.S. Geological Survey, Northborough, MA 01532.*
[c.] *U.S. Geological Survey, Boulder, CO 80303.*
[d.] *Department of Environmental Health, Harvard T. H. Chan School of Public Health, Harvard University, Boston, MA 02115.*

Table of Contents

Site Overview.

Recharge to the unconfined sand and gravel aquifer from precipitation is ~73 cm yr^{-1} and the average groundwater flow velocity is ~0.4 m d^{-1}.[1-3] The groundwater flow direction in the surrounding aquifer is generally from north to south.[4] Ashumet Pond has a maximum depth of 19 m, a volume of 6.26 million m^3,[5] model-simulated total groundwater outflow of 3.81 x 10^6 m^3 $year^{-1}$,[6] and an estimated hydraulic residence time of 1.6 yrs. Rates of volumetric water flux across the lake bottom have been measured at the upwelling (groundwater discharge into lake) and downwelling (lake recharge into the aquifer) porewater sites (Fig. 1B) to be from 0.09 to 1.6 m^3 m^{-2} d^{-1}.[7-9] At downwelling site GWOUT-L-N at Ashumet Pond, the seepage rates were calculated to be approximately 0.62 m d^{-1} (water depth of 0.31 m) and 0.16 m d^{-1} (water depth of 0.62 m) in September/October 2017 and February 2018, respectively.[9] At downwelling site GWOUT-R-N Ashumet Pond, the seepage rates were calculated to be approximately 1.0 m d^{-1} (water depth of 0.33 m) and 0.31 m d^{-1} (water depth of 0.58 m) in September/October 2017 and February 2018, respectively.[9] The lake level varied about 1.1 m during this study (July 2016 to February 2019) and about 1.8 m historically (1972-2019).[10] The lake level in Ashumet Pond was higher during downwelling porewater sampling during the February 2018 (13.8 m) and February 2019 (14.0 m) sampling than during the September 2017 sampling (13.5 m).[10] Data on lake level can be found on the U.S. Geological Survey (USGS) National Water Information System website.[10] Another groundwater-flow-through kettle lake (Johns Pond) is located southeast of Ashumet Pond and has one primary surface outflow (Quashnet River).

Lake, Groundwater, and Sediment Sampling.

Water samples for analysis of per- and polyfluoroalkyl substances (PFAS) were collected in high-density polyethylene (HDPE) bottles with polypropylene or polyethylene caps. Bottles were pre-cleaned with liquid chromatography mass spectrometry (LC-MS) grade methanol and

deionized (DI) water and rinsed 3 times with sample water before filling, except for water samples from 2016 (from near the PFAS plume upgradient from Ashumet Pond), which were rinsed 3 times with only sample water before filling. DI water equipment blanks were collected for sampling equipment (see below) by running DI water through the sampling system. All PFAS water samples were unfiltered, stored on ice in the field, and then stored at 4 °C until analysis. Specific conductance was measured using an Orion Star™ A222 meter (ThermoFisher Scientific, Waltham, MA), and pH was measured with an Orion Star™ A221 meter (ThermoFisher Scientific, Waltham, MA), an Orion™ Ross™ Sure-Flow™ 8172 electrode, and an Orion™ ATC stainless steel temperature-compensating probe (ThermoFisher Scientific, Waltham, MA). Samples with dissolved oxygen (DO) concentrations >31 μM were collected in flushed glass biochemical oxygen demand bottles, stoppered, chilled, and measured within 6 hours with a YSI 58 portable DO meter (Yellow Springs, OH) and YSI 5905 self-stirring biochemical oxygen demand probe (Yellow Springs, OH). DO concentrations <31 μM were measured using a CHEMetrics (Midland, VA) V-2000 photometer and K-7553 Vacu-vial self-filling reagent ampoules. Additional water quality analyses included chloride, sulfate, nitrate, and dissolved organic carbon (DOC), as described elsewhere.[11]

Groundwater samples were collected from monitoring well clusters or multilevel samplers (MLSs) with either a Grundfos RediFlo2™ submersible pump, Keck SP-81™ submersible pump, or a GeoPump2™ (Geotech, Denver, CO) peristaltic pump as previously described.[12] A minimum of three well volumes were purged before sample collection. For MLSs, three volumes from the MLS tubing was purged. Porewater was collected using screened stainless steel pushpoint samplers (MHE Products, East Tawas, MI) attached to the GeoPump2 ™ peristaltic pump outfitted with Norprene™ tubing after purging three times the tubing volume. Lake-water samples were collected using a GeoPump2™ with polyethylene tubing attached to a YSI™ 6920 Multi-

Parameter Water Quality Sonde (Yellow Springs, OH) that was lowered to the desired sampling depth.

Microlayer samples were collected by inserting a 30.5 x 30.5 x 0.5 cm glass plate vertically into the water next to the boat, withdrawing the plate at a rate of ~15 cm sec^{-1}, [13] and using a silicone rubber squeegee blade to capture the water from the plate in HDPE sample containers. Both the blade and glass plate were rinsed with methanol after each sample was collected to prevent cross-contamination. The water surface was generally calm during sampling except during the November 2018 sampling (wind and waves).

Sediment samples were collected as described in the manuscript and transferred to HDPE bottles. Soil samples were collected by scooping into pre-cleaned HDPE bottles after removing any leaf litter and grass. Soil and sediment samples were kept chilled in the field, and stored frozen at -20°C until analysis.

Chemicals and Materials.

DI water with a resistivity of >18 MΩ cm^{-1} was obtained from a GenPure™ xCAD Plus UV-TOC system (Thermo Scientific™ Barnstead™, Lake Balboa, CA). LC-MS grade methanol (J.T. Baker, Center Valley, PA) and ACS grade ammonium hydroxide were purchased from VWR (Radnor, PA). ACS grade hydrochloric acid (HCl) was purchased from Fisher Scientific (Waltham, MA). Reagent grade formic acid, BioUltra ammonium acetate, ACS grade acetic acid, and Supelclean ENVI-Carb (120-400 mesh, 100 m^2 g^{-1} surface area) were obtained from Sigma Aldrich (St. Louis, MO). Oasis WAX cartridges (6 mL, 150 mg, 30 µm particle size) for solid phase extraction (SPE) were obtained from Waters (Milford, MA).

Sample Preparation and LC-MS/MS Analysis.

Water samples were warmed to room temperature, briefly sonicated, and inverted several times before subsampling 20 mL into a 50 mL centrifuge tube. The sample was then spiked with internal standards, extracted using offline SPE, and prepared for analysis as described in the manuscript. LC-MS/MS analysis was conducted as described previously,[12] with minor modifications outlined here. **All PFAS sample data are available in the associated data release**.[14] LC-MS/MS blanks and the calibration curve were prepared with 50:50 methanol:DI water and internal standard concentrations matching the samples. The 11-point calibration curve ranged from 1 to 10,000 ng L^{-1}, and calibration quality controls were included throughout the sample run. Branched and linear PFOS and PFHxS were quantified with individual native isomer calibration curves and summed to obtain the reported totals for PFOS and PFHxS. Initial conditions were 97% 2 mM ammonium acetate in DI water (A) and 3% mM ammonium acetate in methanol (B). From 0.85 to 3.5 min the gradient was linearly increased to 54% B. From 3.5 to 16 min the gradient was linearly increased to 85% B, and then from 16 to 16.5 min the gradient was linearly increased to 100% B and maintained until the end of the run (17.5 min). The column temperature was 50 °C. Mass spectrometry parameters are detailed in Table S2.

TOP Analysis.

A 20 mL water sample was combined with 20 mL of 120 mM potassium persulfate and 250 mM sodium hydroxide aqueous solution in an HDPE bottle and maintained at 85°C overnight in a water bath. Samples were then cooled to room temperature, neutralized with hydrochloric acid, and extracted in the same manner as unoxidized water samples, with the addition of 4 mL of DI water to rinse the sample bottle and cartridge after concentrating the sample. An additional DI water oxidation blank was included in each batch of 12 extracts.

Total estimated precursor concentrations are reported in nanomolar units because the original mass of the precursors before oxidation is unknown.[12, 15, 16] If samples were below the method quantification limit (MQL) prior to oxidation, the value of the MQL was subtracted from

the post-oxidation sample concentration. Note that the term “PFAA precursors” refers to precursors that are oxidized by the TOP assay and/or inferred by Bayesian Inference as described below.

Bayesian Inference Analysis for Total Precursor Concentrations

Bayesian inference is a common statistical procedure used to estimate the conditional probability of an unknown variable given all available observations and their uncertainties. Here, we are able to observe PFCA that are produced during oxidation of unknown precursors in the TOP assay. We use a previously developed[17] Bayesian inference method to infer the sum of the unknown oxidizable precursors (Σ precursors) given concentrations of the terminal PFCA before and after the TOP assay and published laboratory data on oxidative yields and their respective uncertainties[18].

The inference (Eq. 1) predicts the original concentration of Σ precursors (θ) given measured concentrations of oxidation products (x) in the TOP assay:

$$\pi(\theta|x) \propto \pi(\theta)p(x|\theta) \quad \text{(Eq. 1)}$$

where:

$\pi(\theta|x)$ is the posterior, the log10-normal distribution of unknown PFAS concentrations.

$\pi(\theta)$, is the prior, the log10 uncertainty in concentrations of unknown PFAS based on known information regarding the concentrations of these compounds. For all samples, we use noninformative uniform prior U(-6, log(10*$\Sigma_{\text{PFBA (c3)-PFNA(C8)}}$ PFCA produced by the TOP assay)). A noninformative prior was used because of the undetermined biogeochemical processes that alter PFAS composition in downwelling porewater in Ashumet Pond. $p(x|\theta)$ is the likelihood, the log10 sum of least squares estimator:

$$p(x|\theta)=\Sigma_i[(\mu_{A,i}\theta_i-x)/\varepsilon_i]^2 \quad \text{(Eq. 2)}$$

where:

$\mu_{A,i}$ represent the average molar oxidation yields of unknown PFAS i into perfluoroalkyl carboxylates reported in the literature as aggregated in Table S5 of Ruyle et al.[18]. ε_i is the total error of the comparison for PFAS i:

$$\varepsilon_i=[(\sigma_{A,i}/\mu_{A,i})^2 + \Delta_{x,i}^2]^{0.5} \text{ (Eq. 3)}$$

where, σ_{Ai} is the standard deviation of the average molar oxidation yields of unknown PFAS i into perfluoroalkyl carboxylates reported in the literature and $\Delta_{x,i}$ is the relative error in the measurement. For all samples we set $\Delta_{x,i}$ equal to 0.1 as a realistic estimate for the percent difference in the increase in sum PFCA across duplicate samples.

The posterior distribution was sampled by Markov chain Monte Carlo (MCMC) analysis using 32 ensemble samplers using *emcee* 3.0.2[19] in Python 3.7.8. Sequential steps in the Markov chain were determined using the differential evolution algorithm[20] with the mean equal to 0.595 (2.38/SQRT[2*ndim]) and standard deviation equal to 1.01, following the recommendation of the software[19]. The MCMC was run until the Monte Carlo standard error was 1/SQRT(2,500) of the standard deviation of the posterior distribution. The source code and data used for the inference is available for review and use at https://github.com/SunderlandLab/oxidizable-pfas-precursor-inference.

Sediment PFAS and TOP Analysis.

Frozen sediment samples were thawed, subsampled into 50 mL polypropylene centrifuge tubes, and centrifuged at 4,000 rpm for 20 min. The porewater supernatant was transferred to another container and the sediment was dried at 45 °C. The sediment weight before and after drying was recorded to determine the volume of water removed and to allow for calculation of PFAS concentrations in the sediment. The sediment was then sieved through a 2.36 mm sieve and homogenized, and 10 ± 0.05 g (when available) was subsampled into 50 mL polypropylene centrifuge tubes. Each sediment sample was prepared in triplicate. The sediment samples were

mixed with 18 mL of 0.1% ammonium hydroxide in methanol, vortexed briefly, bath sonicated at 40 °C for 30 min, placed on a rotating table for 2 hr, and centrifuged at 4,000 rpm for 20 min, and the supernatant was transferred to a new 50 mL polypropylene centrifuge tube. The methanol extraction was repeated 3 times, and the combined methanolic extracts were dried under an ultra-high purity nitrogen gas stream to ~5 mL before being split into two fractions to allow for analysis of PFAS and PFAA precursors through implementation of the TOP assay.

The first fraction was dried under an ultra-high-purity nitrogen gas stream and reconstituted with 1.5 mL of 0.1 % acetic acid in methanol, heated to 45 °C for 30 min, and vortexed briefly before transfer to a polypropylene microcentrifuge tube containing 25-30 mg of ENVI-Carb to remove dissolved organic matter. The methanol-ENVI-carb samples were vortexed, then centrifuged at 13,000 rpm for 20 min, and 710 µL of methanol supernatant was transferred to a microcentrifuge tube containing 750 µL DI water and 40 µL of a 0.03 ng μL^{-1} internal standard solution. Finally, samples were vortexed and centrifuged at 13,000 rpm for 20 min before the supernatant was transferred to a 1 mL polypropylene vial for LC-MS/MS analysis as previously described.

For the second fraction, 25±5 mg ENVI-Carb was added directly to the centrifuge tubes containing the sediment extract and vortexed. The samples were then filtered using a 0.2 µm polypropylene filter and added to 60 mL HDPE bottles. The methanolic extracts were then dried using nitrogen gas and reconstituted with 20 mL DI water. The samples were then oxidized and extracted with offline SPE following the TOP assay procedure described above.

Sediment Metal Analysis.

A total of 5±0.2 g of dried sediment (prepared as described previously) was weighed out into 50 mL polypropylene centrifuge tubes, covered with aluminum foil, and extracted with 40 mL 0.5 M HCl for 3 d on a rotating shaker table.[21, 22] The extracts were then centrifuged at 4,000 rpm for 10 min, and the supernatant was filtered with a 0.45 µm polyvinylidene fluoride (PVDF) filter.

Samples were diluted with 2% nitric acid, and scandium (Sc), yttrium (Y), and terbium (Tb) internal standards were added. Analysis was completed with a Thermo iCAP Q (Waltham, MA) inductively coupled plasma mass spectrometer (ICPMS). Sediment concentrations are reported in Table S9, and average recoveries of the NIST 1643f standard containing trace elements in water are reported in Table S10. Table S11 reports the average relative percent difference (RPD) and standard deviation for analytical duplicate samples, and Table S12 contains the relative standard deviation (RSD) (%) for samples digested and analyzed in triplicate.

Extractable Organofluorine (EOF) Analysis.

A boat blank was run between each set of duplicate injections of 100 µL. Peak areas were subtracted from the boat blanks, and the residual standard deviations of duplicate injections were <9%. Concentrations were determined from the average peak areas of duplicate injections using a nine-point calibration curve from 50 to 10,000 ug F L-1 ($R2 > 0.999$; F as fluoride, ERA-IC1035 Custom Anion Mix, Metrohm) in LCMS-grade MeOH. The limit of detection (LOD), 270 µg F L^{-1}, was determined from the average plus three times the standard deviation of the peak area of the Milli-Q water extraction blank. Concentrations above the LOD were adjusted by the dilution factor and reported here.

Quality Assurance and Quality Control.

Water Sample Analysis. DI water SPE blanks for non-oxidized water analysis were <MQL for all compounds, except for PFBA and 6:2 FtS. Because 6:2 FtS had large fluctuations in blank concentrations, it was excluded from the analysis, and was only used during the TOP assay as a precursor spike to ensure precursors were degraded. The issue with 6:2 FtS appeared to originate during the SPE stage, as blanks extracted for sediment (see below) did not have any detections. PFBA was blank-corrected using the mean quantified concentrations of the SPE DI water blanks

(2.96 ng L^{-1}), and the MQL was set to the mean plus three times the standard deviation of the SPE DI blanks. The MDL was three times less than the MQL. For all other compounds, the MDLs and MQLs were the average sample concentrations at which the signal-to-noise ratio was 3 and 10, respectively. All field equipment blanks (*n*=5 peristaltic pump, *n*=1 Grundfos pump, *n*=1 Keck pump, *n*=3 pushpoint samplers, *n*=1 microlayer sampler, and 3 wader DI water blanks) were below the MQL, except for the blanks taken by running DI water over waders used in lake sampling. These wader blanks produced low levels of PFAS (<3 ng L^{-1}) and were at least 16 times lower in concentration than PFAS in Ashumet Pond samples on an individual compound basis, except for N-EtFOSAA, which was detected at 1.3 ng L^{-1} in the waders but not in Ashumet Pond samples, and therefore was not a concern. Average recoveries of DI water spiked with 7.5 ng L^{-1}, 75 ng L^{-1}, or 750 ng L^{-1} native PFAS ranged from 89.9% to 125%, and the percent relative standard deviation ranged from 2.96% to 20.0% (Table S3). Average recoveries for samples spiked with 75 ng L^{-1} native PFAS ranged from 91.4% to 107%, and the percent relative standard deviation ranged from 5.6% to 17.3% (Table S3). For SPE sample duplicates (*n*=46, also known as split replicates), the average relative percent difference (RPD) ranged from 3.0%-31% depending on the compound, and the maximum RPD for any compound in any sample was 31% (PFNS). For field duplicates (*n*=31, also known as sequential replicates), the average RPD ranged from 3.5%-19% depending on the compound, and the maximum RPD for any compound in any sample was 46.4% (n-PFOS). RPD calculations include only compounds over the MQL and qualifiers within range (±30%).

TOP Analysis. TOP samples were blank-corrected using the average quantified concentration of the oxidation blanks for PFBA (4.56 ng L^{-1}), PFPeA (1.70 ng L^{-1}), PFHxA (3.18 ng L^{-1}), and PFHpA (1.17 ng L^{-1}). All other compounds were below the MQL in DI water oxidation blanks and SPE DI water blanks. The MQLs and MDLs for compounds with blank correction were calculated as described above. All field equipment blanks were below the MQL except for a blank taken after sampling Ashumet Pond in November 2018, which produced PFBA concentrations of 14 ng L^{-1}

after oxidation. All conclusions in the manuscript were re-evaluated using precursor concentrations calculated only from PFPeA and PFHxA increases after oxidation (eliminating PFBA), and were found to be the same. To evaluate spike recoveries for the oxidized matrix, DI water and samples used for spike recoveries were first oxidized along with all other samples before adding a spike of native PFAS before SPE extraction. Native PFAS were added after oxidation to prevent degradation of the PFAA precursors in the native spike. Average recoveries of oxidized DI water spiked with 7.5 ng L^{-1}, 75 ng L^{-1}, or 750 ng L^{-1} native PFAS after oxidation ranged from 76.2% to 124%, and the RSD ranged from 1.10% to 34.2% (Table S4). Average recoveries for oxidized samples spiked with 75 ng L^{-1} native PFAS after oxidation ranged from 85.1% to 112%, and the RSD ranged from 4.26% to 21.1% (Table S4). For oxidized sample duplicates (n=12), the average RPD ranged from 1.3%-9.3% for any one compound, and the maximum RPD for any compound in any sample was 35% (br-PFHxS). RPD calculations include only compounds over the MQL and qualifiers within range (±30%). To ensure precursors were degraded during the oxidation experiments, a groundwater sample and a lake-water sample were spiked in triplicate with 3 ng of 6:2 FtS, 8:2 FtS, N-MeFOSAA, N-EtFOSAA, and FOSA. Precursor concentrations were all reduced by >95%, and the molar recovery of PFAS was between 93% and 104%.

Following the TOP assay, there were no detections above the LOQ for any of the quantified precursor compounds (4:2 FtS, 8:2 FtS, N-MeFOSAA, N-EtFOSAA, and FOSA) even for samples that had detections of one or more of these compounds pre-oxidation.

Sediment Analysis. Empty centrifuge tubes (n = 4) were extracted alongside the sediments, and all results were below the quantification limit. To test recoveries, one sample (GWOUT-L-N 17 – 32 cm, collected in September 2017), was spiked with 9 ng of all native PFAS, left to equilibrate for 24 hr at room temperature, and extracted following the same method as all other sediment and blank samples. Average recoveries ranged from 68.6% (PFTrDA) to 95.2% (PFHpS) as

shown in Table S4. Two samples were sequentially extracted four times, but a fourth extraction was not necessary to improve PFAS recovery (Fig. S13).[14]

For the sediment extracts subjected to the TOP assay, three blank extracts were included for quality control; all were <MQL. Precursors (4:2 FtS, 6:2 FtS, 8:2 FtS, N-MeFOSAA, N-EtFOSAA, and FOSA) originally in the 9 ng native PFAS spike described in the above paragraph were degraded by >95% as a result of oxidation. An additional 3 blanks were included during offline SPE and were also all <MQL. Recoveries from samples spiked with 1.5 ng native PFAS directly before offline SPE are shown in Table S6.

EOF Analysis. The percent difference of duplicate extractions of Ashumet Pond water was 16%. Recovery of a 330 µg F L^{-1} as perfluorooctanoate (PFOA, 95% purity, Sigma-Aldrich, St. Louis, MO) spike was 101% in Milli-Q water and 74% in a sample. The percent recovery of the PFOA spike measured on the LC-MS/MS was 94% in Milli-Q water and 67% in the sample, indicating some loss of PFOA during the extraction rather than incomplete combustion.

PFAS in the Lake-Water Microlayer.

PFAS enrichment factors in Ashumet Pond (*n*=5) and Johns Pond (*n*=7) were calculated at each sampling location by dividing the microlayer concentration by the concentration in samples taken 10 cm below the lake surface. Samples were considered enriched in PFAS if the enrichment factor exceeded 1.2. PFOS concentrations were enriched in three of the five Ashumet Pond microlayer samples (top ~50 µm[13]) by 1.6 ± 0.19 (mean ± standard deviation) times (Fig. 3B). Individually, linear and branched PFOS concentrations were enriched 1.7 ± 0.21 and 1.4 ± 0.15 times for the three samples, respectively. PFNA was enriched 1.4 times in 1 Ashumet Pond sample location. No microlayer enrichment was observed for any other PFAS in Ashumet Pond. In Johns Pond (*n*=2 microlayer samples collected), total PFOS was enriched 2.5 ± 1.6 times (*n*=2), linear PFOS was enriched 2.8 ± 1.8 times (*n*=2), branched PFOS was enriched 2.6 (*n*=1) times,

PFNA was enriched 1.8 times (*n*=1), and perfluoroheptane sulfonate (PFHpS) was enriched 1.3 times (*n*=1). Enrichment was only observed for long chain-length PFAA ($\eta_{pfc} \geq 7$ for PFCA and $\eta_{pfc} \geq 6$ for PFSA[23]), which agrees with previous work indicating that air-water partitioning is greater for compounds with a longer perfluoroalkyl chain length.[24, 25]

Tables

Table S1. Water levels in selected wells downgradient from Ashumet Pond (F is shorthand for MA-FSW).[10]

Well	USGS Site ID	Date of Water Level	Water-Level Depth Below Land Surface (feet)	Land-Surface Elevation (feet above NGVD29)	Water-Level Elevation (feet above NGVD29)
F722-0014	413735070320731	9/15/2017	6.80	49.23	42.43
F722-0014	413735070320731	2/22/2018	5.80	49.23	43.43
F631-0031	413734070320616	9/15/2017	11.65	53.65	42.00
F631-0031	413734070320616	2/22/2018	10.71	53.65	42.94
F665-0040	413732070320502	9/12/2017	15.35	56.44	41.09
F632-0195	413724070315917	9/11/2017	25.45	65.71	40.26
F632-0195	413724070315917	2/22/2018	24.57	65.71	41.14

Table S2. Per- and polyfluoroalkyl substances (PFAS) analysis tandem mass spectrometry parameters. The Agilent MassHunter Optimizer program was used to optimize product ions, fragmentor voltages, and collision energies.

Analyte Abbrev.	Analyte Name	Type	Internal Standard	Precursor Ion	Product Ion (Quantifier)	Quantifier Collision Energy (V)	Product Ion (Qualifier)	Qualifier Collision Energy (V)	Fragmentor Voltage (V)
Perfluorinated Carboxylates									
PFBA	Perfluorobutanoate	Target	[$^{13}C_4$] PFBA	213	169	2			60
PFPeA	Perfluoropentanoate	Target	[$^{13}C_5$] PFPeA	263	219	2			60
PFHxA	Perfluorohexanoate	Target	[$^{13}C_5$] PFHxA	313	269	2	119		70
PFHpA	Perfluoroheptanoate	Target	[$^{13}C_4$] PFHpA	363	319	2	169/119	10/18	70
PFOA	Perfluorooctanoate	Target	[$^{13}C_8$] PFOA	413	369	2	169	10	80
PFNA	Perfluorononanoate	Target	[$^{13}C_9$] PFNA	463	419	2	219/169	10/14	75
PFDA	Perfluorodecanoate	Target	[$^{13}C_6$] PFDA	513	469	6	269/219	14/14	85
PFUnDA	Perfluoroundecanoate	Target	[$^{13}C_7$] PFUnDA	563	519	6	269/169	14/22	95
PFDoDA	Perfluorododecanoate	Target	[$^{13}C_2$] PFDoDA	613	569	6	269/169	14/26	90
PFTrDA	Perfluorotridecanoate	Target	[$^{13}C_2$] PFDoDA	663	619	6	169	26	95
PFTeDA	Perfluorotetradecanoate	Target	[$^{13}C_2$] PFTeDA	713	669	6	169	25	100
Perfluorinated Sulfonates									
PFBS	Perfluorobutane sulfonate	Target	[$^{13}C_3$] PFBS	299	80	38	99	30	95
PFPeS	Perfluoropentane sulfonate	Target	[$^{13}C_3$] PFHxS	349	80	38	99	30	140
PFHxS	Perfluorohexane sulfonate	Target	[$^{13}C_3$] PFHxS	399	80	58	99	34	135
PFHpS	Perfluoroheptane sulfonate	Target	[$^{13}C_8$] PFOS	449	80	54	99	42	180
PFOS	Perfluorooctane sulfonate	Target	[$^{13}C_8$] PFOS	499	80	60	99	50	200
PFNS	Perfluorononane sulfonate	Target	[$^{13}C_8$] PFOS	549	80	60	99	54	175
PFDS	Perfluorodecane sulfonate	Target	[$^{13}C_8$] PFOS	599	80	60	99	54	175
Fluorotelomer Sulfonates									
4:2 FtS	4:2 fluorotelomer sulfonate	Target	[$^{13}C_2$] 4:2 FtS	327	307	10	81	30	130
6:2 FtS	6:2 fluorotelomer sulfonate	Target	[$^{13}C_2$] 6:2 FtS	427	407	18	81	34	135
8:2 FtS	8:2 fluorotelomer sulfonate	Target	[$^{13}C_2$] 8:2 FtS	527	507	26	81	42	180

Analyte Abbrev.	Analyte Name	Type	Internal Standard	Precursor Ion	Product Ion (Quantifier)	Quantifier Collision Energy (V)	Product Ion (Qualifier)	Qualifier Collision Energy (V)	Fragmentor Voltage (V)
Perfluoroalkyl Sulfonamides									
FOSA	Perfluorooctane sulfonamide	Target	[$^{13}C_8$] FOSA	498	78	38			140
Perfluoroalkyl Sulfonamidoacetates									
N-EtFOSAA	N-Ethyl perfluorooctane sulfonamidoacetate	Target	d5-N-EtFOSAA	584	419	18	526	14	95
N-MeFOSAA	N-Methyl perfluorooctane sulfonamidoacetate	Target	d3-N-MeFOSAA	570	419	14	483	10	95
Internal Standards									
[$^{13}C_4$] PFBA		ISTD		217	172	2			60
[$^{13}C_5$] PFPeA		ISTD		268	223	2			60
[$^{13}C_5$] PFHxA		ISTD		318	273	2			70
[$^{13}C_4$] PFHpA		ISTD		367	322	2			70
[$^{13}C_8$] PFOA		ISTD		421	376	2			75
[$^{13}C_9$] PFNA		ISTD		472	427	2			85
[$^{13}C_6$] PFDA		ISTD		519	474	2			90
[$^{13}C_7$] PFUnDA		ISTD		570	525	6			85
[$^{13}C_2$] PFDoDA		ISTD		615	570	6			95
[$^{13}C_2$] PFTeDA		ISTD		715	670	6			95
[$^{13}C_3$] PFBS		ISTD		302	99	26			95
[$^{13}C_3$] PFHxS		ISTD		402	99	38			180
[$^{13}C_8$] PFOS		ISTD		507	99	50			180
[$^{13}C_2$] 4:2 FtS		ISTD		329	81	38			95
[$^{13}C_2$] 6:2 FtS		ISTD		429	81	46			95
[$^{13}C_2$] 8:2 FtS		ISTD		529	81	46			180
[$^{13}C_8$] FOSA		ISTD		506	78	38			95
d5-N-EtFOSAA		ISTD		589	419	14			95
d3-N-MeFOSAA		ISTD		573	419	14			100

Table S3. Average recovery (%) and relative standard deviation (RSD, %) for deionized water (DI H_2O) spiked with 7.5 ng L^{-1}, 75 ng L^{-1}, and 750 ng L^{-1} of the native per- and polyfluoroalkyl substances (PFAS) standards and environmental samples spiked with 75 ng L^{-1} native PFAS standards (matrix spike). Branched and linear isomers are denoted by br- and n-, respectively. N/A indicates no recovery or RSD could not be calculated because spike was below the method quantification limit (MQL).

Analyte	7.5 ng L^{-1} DI H_2O Spike (*n* = 8)		75 ng L^{-1} DI H_2O Spike (*n* = 8)		750 ng L^{-1} DI H_2O Spike (*n* = 7)		75 ng L^{-1} Matrix Spike (*n* = 23)	
	Recovery (%)	RSD (%)	Recovery (%)	RSD (%)	Recovery (%)	RSD (%)	Recovery (%)	RSD (%)
PFBA	125.1	3.8	103.9	6.9	99.5	3.5	106.6	6.2
PFPeA	109.1	8.8	104.0	5.1	99.7	3.7	103.3	6.0
PFHxA	103.6	9.2	104.3	5.4	100.8	3.7	104.6	5.6
PFHpA	104.2	8.5	103.6	7.4	100.7	3.7	103.6	6.9
PFOA	103.8	9.2	102.8	6.5	100.3	3.6	103.3	6.1
PFNA	106.4	9.5	103.7	5.6	101.0	3.0	103.5	5.8
PFDA	102.4	9.6	102.2	5.9	99.2	4.8	102.7	5.8
PFUnDA	104.8	9.0	104.4	6.5	99.1	5.2	103.7	5.9
PFDoDA	105.5	9.8	104.3	7.6	100.1	4.1	103.1	7.0
PFTrDA	108.2	13.3	108.5	7.2	106.2	5.5	101.5	11.7
PFTeDA	107.2	8.1	104.6	6.5	100.0	3.5	103.9	5.6
PFBS	107.6	9.6	103.9	7.6	97.5	4.0	107.1	6.2
PFPeS	123.4	20.0	109.3	6.1	121.1	15.1	101.9	13.2
n-PFHxS	119.8	14.7	110.3	7.2	107.0	11.1	100.2	13.9
br-PFHxS	N/A	N/A	100.2	8.7	97.2	5.2	95.3	14.7
PFHpS	103.2	11.1	104.9	6.0	101.9	3.3	106.1	7.8
n-PFOS	110.0	9.2	104.8	7.4	99.6	3.5	103.4	7.6
br-PFOS	109.0	8.1	92.8	13.2	89.9	3.6	92.3	12.2
PFNS	101.5	7.7	100.4	9.1	95.6	4.1	101.0	9.2
PFDS	102.2	12.3	100.8	8.3	95.5	3.0	100.4	11.5
4:2 FtS	101.8	13.3	101.3	7.8	97.5	6.1	105.7	8.7
8:2 FtS	109.0	11.1	103.0	6.1	100.9	7.1	104.6	6.7
N-MeFOSAA	99.6	13.1	105.4	8.4	96.1	8.7	101.8	9.0
N-EtFOSAA	108.9	14.7	104.6	12.1	90.9	8.6	100.6	11.9
FOSA	94.3	15.9	91.3	19.5	94.0	8.1	91.4	17.3

Table S4. Average recovery (%) and relative standard deviation (RSD, %) for deionized water (DI H_2O) spiked with 7.5 ng L^{-1}, 75 ng L^{-1}, and 750 ng L^{-1} native per- and polyfluoroalkyl substances (PFAS) standards following total oxidizable precursor assay oxidation and environmental samples spiked with 75 ng L^{-1} native PFAS standards (matrix spike) following total oxidizable precursor assay oxidation. Branched and linear isomers are denoted by br- and n-, respectively. N/A indicates no recovery or RSD could not be calculated because spike was below the method quantification limit (MQL) or because there was only 1 value above the MQL.

Analyte	7.5 ng L^{-1} DI H_2O Spike (*n* = 3)		75 ng L^{-1} DI H_2O Spike (*n* = 2)		750 ng L^{-1} DI H_2O Spike (*n* = 2)		75 ng L^{-1} Matrix Spike (*n* = 6)	
	Recovery (%)	RSD (%)	Recovery (%)	RSD (%)	Recovery (%)	RSD (%)	Recovery (%)	RSD (%)
PFBA	N/A	N/A	105.8	1.3	110.9	5.7	112.2	9.7
PFPeA	108.3	18.4	111.9	13.2	111.7	7.3	108.4	4.3
PFHxA	N/A	N/A	107.2	13.0	108.0	6.3	110.6	6.6
PFHpA	100.0	4.0	106.7	11.6	112.6	5.6	106.3	7.1
PFOA	110.4	5.0	106.7	13.0	110.1	4.8	108.9	6.3
PFNA	107.2	5.3	109.6	10.4	109.5	5.2	108.4	4.6
PFDA	105.7	2.3	104.8	11.4	112.1	3.6	108.8	5.2
PFUnDA	106.3	4.6	105.8	10.0	109.8	5.2	107.1	5.7
PFDoDA	104.8	2.9	108.2	10.4	111.3	5.5	107.4	6.2
PFTrDA	95.7	17.2	109.4	14.1	110.3	14.5	104.1	14.7
PFTeDA	109.6	5.4	106.6	9.2	109.3	4.8	108.1	6.4
PFBS	105.4	11.2	102.4	8.7	111.7	5.4	107.2	5.0
PFPeS	103.4	11.0	100.1	8.3	120.8	6.7	105.5	16.7
n-PFHxS	107.4	3.8	112.6	6.8	110.8	8.1	104.0	12.0
br-PFHxS	N/A	N/A	97.7	7.2	89.8	3.7	91.1	12.5
PFHpS	102.8	14.9	99.4	25.0	124.4	25.4	102.0	13.8
n-PFOS	105.5	5.7	103.4	14.3	119.5	20.3	105.9	10.0
br-PFOS	120.7	N/A	76.2	34.2	98.0	9.8	85.1	21.1
PFNS	88.0	17.1	92.8	25.1	113.2	18.7	97.1	15.3
PFDS	100.1	9.6	97.3	23.1	112.7	24.4	103.1	10.6
4:2 FtS	103.1	9.3	104.8	9.2	106.3	7.6	108.3	4.8
8:2 FtS	101.1	5.5	100.0	12.4	111.9	17.0	105.4	6.7
N-MeFOSAA	102.4	4.4	104.7	14.0	109.7	3.2	106.8	7.3
N-EtFOSAA	92.4	13.1	107.2	13.7	118.2	1.1	103.6	9.8
FOSA	92.2	6.0	97.6	2.3	105.7	1.9	101.7	7.4

Table S5. Average recovery (%) and relative standard deviation (RSD, %) for sediment samples spiked with 9 ng native per- and polyfluoroalkyl substances (PFAS) prior to sediment extraction. Branched and linear isomers are denoted by br- and n-, respectively.

Analyte	Recovery (%) (n = 3)	RSD (%)
PFBA	82.1	3.2
PFPeA	79.7	9.8
PFHxA	79.0	13.5
PFHpA	82.4	4.5
PFOA	76.0	16.4
PFNA	83.2	3.2
PFDA	82.3	1.8
PFUnDA	77.6	12.1
PFDoDA	85.3	1.7
PFTrDA	68.6	5.4
PFTeDA	82.4	3.0
PFBS	88.6	4.8
PFPeS	84.6	1.9
n-PFHxS	84.2	3.8
br-PFHxS	76.4	9.3
PFHpS	95.2	2.2
n-PFOS	70.8	29.7
br-PFOS	79.8	13.0
PFNS	88.1	4.3
PFDS	76.1	1.4
4:2 FtS	85.2	3.8
8:2 FtS	86.8	2.5
N-MeFOSAA	75.3	4.7
N-EtFOSAA	70.8	1.4
FOSA	81.7	4.4

Table S6. Average recovery (%) for sediment samples spiked with 1.5 ng native per- and polyfluoroalkyl substances (PFAS) prior to offline solid phase extraction and post total oxidizable precursor assay. Branched and linear isomers are denoted by br- and n-, respectively. Poor and over-recoveries for linear perfluorooctane sulfonate (PFOS) for both spike samples and perfluoroundecanoate (PFUnDA) for GWIN-124N 0-5 cm are likely due to the high native concentration in the sediment compared to the spike concentration.

Analyte	GWOUT-L-N 17-32 cm Recovery (%)	GWIN-124N 0-5 cm Recovery (%)
PFBA	104	112
PFPeA	114	129
PFHxA	105	141
PFHpA	94	126
PFOA	84	123
PFNA	101	126
PFDA	107	120
PFUnDA	89	234
PFDoDA	102	118
PFTrDA	94	107
PFTeDA	103	116
PFBS	101	125
PFPeS	96	108
n-PFHxS	117	148
br-PFHxS	89	125
PFHpS	113	144
n-PFOS	43	240
br-PFOS	76	185
PFNS	118	148
PFDS	112	138
4:2 FtS	97	125
8:2 FtS	96	112
N-MeFOSAA	93	119
N-EtFOSAA	103	119
FOSA	103	119

Table S7. Average sediment concentration pre- total oxidizable precursor (TOP) oxidation, and average additional concentration produced from the TOP assay in nanograms per kilogram. The additional concentration produced from the TOP assay is the concentration difference between sediment samples pre- and post-TOP oxidation.

			Concentration (ng kg^{-1})						
Sample	**Collection Date**	**# Replicates**	**PFBA**	**PFPeA**	**PFHxA**	**PFHpA**	**PFOA**	**PFNA**	**PFDA**
Average Pre-TOP Oxidation Sediment Concentration									
GWOUT-L-N 0-5 cm	Sept. 2017	3	46.3	213.3	235.5	124.5	500.2	117.4	14.3
GWOUT-L-N 17-32 cm	Sept. 2017	3	275.7	425.1	672.7	416.2	1270.9	186.6	14.7
GWOUT-R-N 0-5 cm	Sept. 2017	3	43.4	222.5	300.3	314.5	2788.7	981.8	80.5
GWIN-124N 0-5 cm	Sept. 2017	3	<MQL	31.8	67.6	18.0	62.6	184.2	19.6
GWIN-124N 15-30 cm	Sept. 2017	3	<MQL	<MQL	<MQL	3.5	12.2	43.7	<MQL
GWOUT-R-S 0-5 cm	Feb. 2019	3	<MQL	98.3	96.9	83.2	659.1	189.4	23.6
GWOUT-R-S 15-30 cm	Feb. 2019	3	130.2	764.6	814.4	272.7	435.6	79.4	13.2
Average Additional Concentration Produced from TOP Assay									
GWOUT-L-N 0-5 cm	Sept. 2017	3	0	45.3	84.4	19.9	105.5	28.3	17.9
GWOUT-L-N 17-32 cm	Sept. 2017	3	0	0	11.2	0	0	0	11.1
GWOUT-R-N 0-5 cm	Sept. 2017	2	0	13.0	62.8	0	71.3	29.1	58.7
GWIN-124N 0-5 cm	Sept. 2017	3	49.8	130.2	230.6	127.1	651.6	0	20.2
GWIN-124N 15-30 cm	Sept. 2017	3	0	33.0	80.0	15.8	162.6	12.1	43.5
GWOUT-R-S 0-5 cm	Feb. 2019	3	51	47.5	122.4	18.4	155.4	64.2	39.7
GWOUT-R-S 15-30 cm	Feb. 2019	3	0	0	0	0	0	0	8.5

Table S8. Sediment/water distribution coefficients (K_d) for upwelling (GWIN) and downwelling (GWOUT) sites. Water sampling site locations shown in Fig.1 correspond to sediment sample locations with the same name. Cells are blank if no K_d value could be calculated because the sediment or water concentration was below the quantification limit. Water and sediment concentrations used to calculate the K_d values are provided in the data release.[14]

		K_d Value (L kg^{-1})*												
Sample	**Collection Date**	**PFBA**	**PFPeA**	**PFHxA**	**PFHpA**	**PFOA**	**PFNA**	**PFDA**	**PFUA**	**PFBS**	**PFPeS**	**PFHxS**	**PFHpS**	**PFOS**
GWOUT-L-N 0-5 cm	Sept. 2017	5.78	13.49	9.54	9.60	14.85	37.16					0.91		15.59
GWOUT-L-N 17-32 cm	Sept. 2017	21.83	21.55	23.04	27.20	30.62	42.89			3.73	3.49	4.17	4.52	22.00
GWOUT-R-N 0-5 cm	Sept. 2017		13.88	12.16	25.02	85.65	327.26					0.90		18.26
GWOUT-R-N 15-30 cm	Sept. 2017	5.08	14.22	15.89	15.94	13.57	15.61		208.56		1.35	1.80		18.91
GWIN-124N 0-5 cm	Sept. 2017		1.30	1.60	0.92	0.98	30.70		791.25			0.63	1.48	11.21
GWIN-124N 15-30 cm	Sept. 2017				0.17	0.25	1.72		10.33			0.91		1.68
GWIN-131N 0-5 cm	Sept. 2017		1.09	1.01	0.72	0.86	12.52		308.32			0.26	0.89	5.92
GWIN-131N 15-30 cm	Sept. 2017		0.25		0.22	0.29	1.17	2.58	14.96			0.65		1.38
GWOUT-R-S 0-5 cm	Feb. 2019		6.47	4.33	7.38	19.98	73.42					0.57	2.93	18.64
GWOUT-R-S 15-30 cm	Feb. 2019	8.14	13.80	10.34	7.58	5.11	8.56		72.78			1.04	1.68	9.44
GWOUT-L-S 0-5 cm	Feb. 2019		3.91	1.98	2.39	4.52	15.30					0.55		19.14
GWOUT-L-S 15-30 cm	Feb. 2019	4.25	6.87	4.25	2.62	3.60	11.21		147.27			0.86	2.07	15.55
GWOUT-0007-C-N 0-5 cm	Feb. 2019		3.49		1.64	1.49	3.43					0.24		6.60
GWOUT-0007-C-N-15 30 cm	Feb. 2019		2.66	5.52	1.94	0.80	4.09					0.12		2.03

*K_d values were calculated using the following pairings between water and sediment: K_d values for the 0-5 cm depth interval were calculated with the lake-water concentration at the sample location (ng L^{-1}) and 0-5 cm depth sediment sample (ng kg^{-1}); K_d values for the 15–30 cm depth interval were calculated with the average porewater concentration from 15 cm and 30 cm and sediment from 15-30 cm depth (GWOUT-L-N was from 17-32 cm depth). Depth is relative to the lake bottom.

Table S9. Inductively coupled plasma mass spectrometry results of aluminum (Al), chromium (Cr), manganese (Mn), iron (Fe), nickel (Ni), copper (Cu), zinc (Zn), and lead (Pb) (µg g^{-1}) extracted from sediment with 40 mL 0.5 M hydrochloric acid over 3 days. All samples are from September 2017.

Sediment Extracted (g)	Sample	Sediment Depth (cm)	Al	Cr	Mn	Fe	Ni	Cu	Zn	Pb
4.87	GWOUT-R-N	0 - 5	154	0.145	49.3	164	0.244	0.364	1.30	2.21
5.12	GWOUT-R-N	15 - 30	481	0.459	18.4	84.4	0.295	0.381	1.53	2.14
5.1	GWOUT-L-N	0 - 5	195	0.268	55.4	181	0.312	0.337	1.94	1.94
4.83	GWOUT-L-N	17 - 32	300	0.282	4.33	113	0.267	0.281	1.32	0.909
5.16	GWIN-131N	0 - 5	186	0.377	1710	1010	0.473	0.456	1.22	3.48
5.07	GWIN-131N	15 - 30	216	0.087	181	119	0.243	0.257	0.264	2.25
4.92	GWIN-124N	0 - 5	211	0.301	1950	285	1.19	1.26	1.23	29.2
5.19	GWIN-124N	15 - 30	161	0.050	32.7	29.0	0.404	0.537	0.0993	0.304

Table S10. Average recoveries and standard deviation for NIST 1643f standard (diluted in deionized water).

	Al (*n*=3)	Cr (*n*=3)	Mn (*n*=4)	Fe (*n*=4)	Ni (*n*=3)	Cu (*n*=4)	Zn (*n*=4)	Pb (*n*=3)
NIST 1643f Concentration (µg L^{-1})	--	0.176	--	--	0.891	--	--	0.176
Average Recovery	--	101.3%	--	--	102.6%	--	--	82.7%
Standard Deviation	--	6.8%	--	--	2.3%	--	--	2.9%
NIST 1643f Concentration (µg L^{-1})	--	18.5	37.1	93.4	59.8	21.7	74.4	18.5
Average Recovery	99.0%	96.4%	94.1%	99.4%	95.9%	98.2%	95.1%	90.7%
Standard Deviation	2.1%	1.0%	1.3%	1.4%	1.1%	0.9%	0.3%	1.1%

Table S11. Average relative percent difference (RPD) and standard deviation for analytical duplicate samples.

	Al (*n*=4)	Cr (*n*=4)	Mn (*n*=2)	Fe (*n*=2)	Ni (*n*=4)	Cu (*n*=2)	Zn (*n*=2)	Pb (*n*=4)
Average Analytical RPD	0.6%	2.4%	1.6%	0.5%	0.7%	0.1%	1.1%	0.9%
Standard Deviation	0.6%	0.6%	0.1%	0.3%	1.0%	0.1%	0.3%	0.3%

Table S12. Relative standard deviation (RSD %) for samples digested and analyzed in triplicate.

		RSD for Triplicate Sample Digestions							
Sample	Sediment Depth (cm)	Al	Cr	Mn	Fe	Ni	Cu	Zn	Pb
GWOUT-R-N	0 - 5	11.6%	11.9%	12.5%	16.8%	11.4%	13.4%	14.9%	15.6%
GWOUT-L-N	12 - 17	6.0%	5.2%	2.6%	3.6%	3.9%	5.5%	3.8%	3.4%

Table S13. Extractable organofluorine concentrations in selected samples.

Sample	Sampling date	EOF [nM F]
MA-FSW 722-M02-05BKT	9/13/2017	8.74
MA-FSW 722-M01-06WT	9/13/2017	2.29
MA-FSW 722-M01-08GY	2/23/2018	4.60
MA-FSW 722-M02-05BKT	2/23/2018	60.73
MA-FSW 722-M02-05BKT	2/14/2019	34.21
FS-ASHPD-0001 (ECAMP02) 5.00m	9/11/2017	29.10
FS-ASHPD-0001 (ECAMP02) 5.00m Duplicate	9/11/2017	34.17
MA-FSW 424-M02-11GN 72-13	7/26/2016	269.38
PFAS DI Blank-MLS Peristaltic Pump	2/22/2018	<LOD

Table S14. Darcy flux and porewater velocity at downwelling and upwelling zones of Ashumet Pond, as reported from various sources.[7-9, 26]

Darcy Flux ($cm^3/cm^2/day$)[a]	Porewater Velocity (cm/day)[b]	Lake-Water Depth (cm)	Source
Downwelling Zone (GWOUT)			
32.4	83	~50	Stoliker et al., 2016
170	436	50	Harvey et al., 2015
26	67	50	Harvey et al., 2015
46	118	25	Hull et al., 2019
162	415	25	Hull et al., 2019
Upwelling Zone (GWIN, where plume discharges)			
10.3	26	~50	Stoliker et al., 2016
8.6	22	not measured	Smith et al., 2019
10.1	26	57	Smith et al., 2019
17.5	45	38	Smith et al., 2019
24.5	63	13.5	Smith et al., 2019
29.0	74	15	Smith et al., 2019
13.0	33	40	Smith et al., 2019

[a] Darcy flux measurements made at different points within each zone
[b] Porewater velocity calculation assumes an effective porosity of 0.39.[7]

Figures

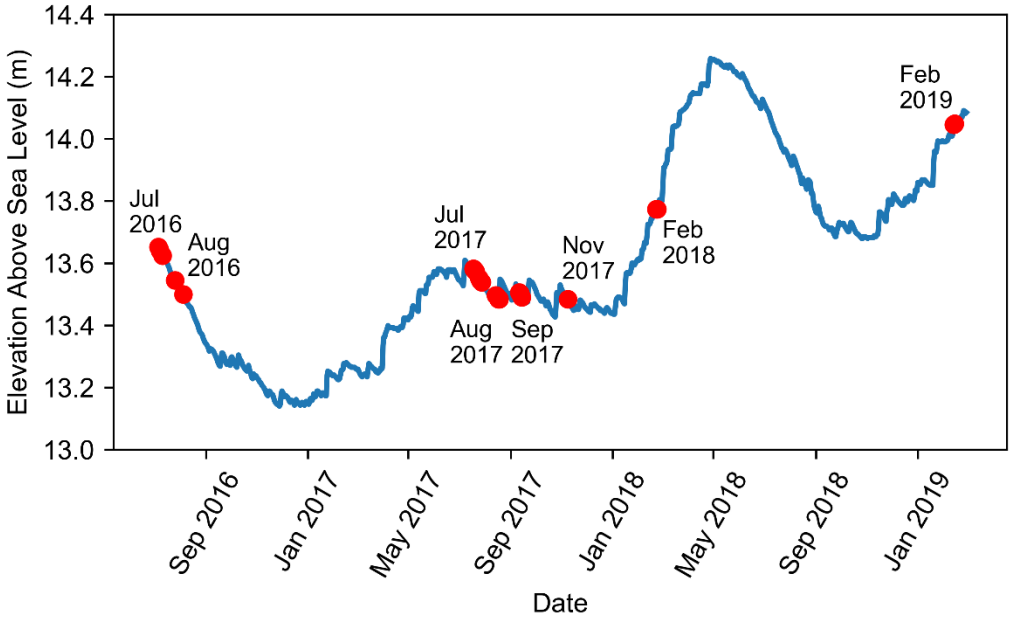

Fig. S1 Water-level elevation above sea level (daily averages) in Ashumet Pond during the sampling period.[10] Red markings indicate times when samples were collected.

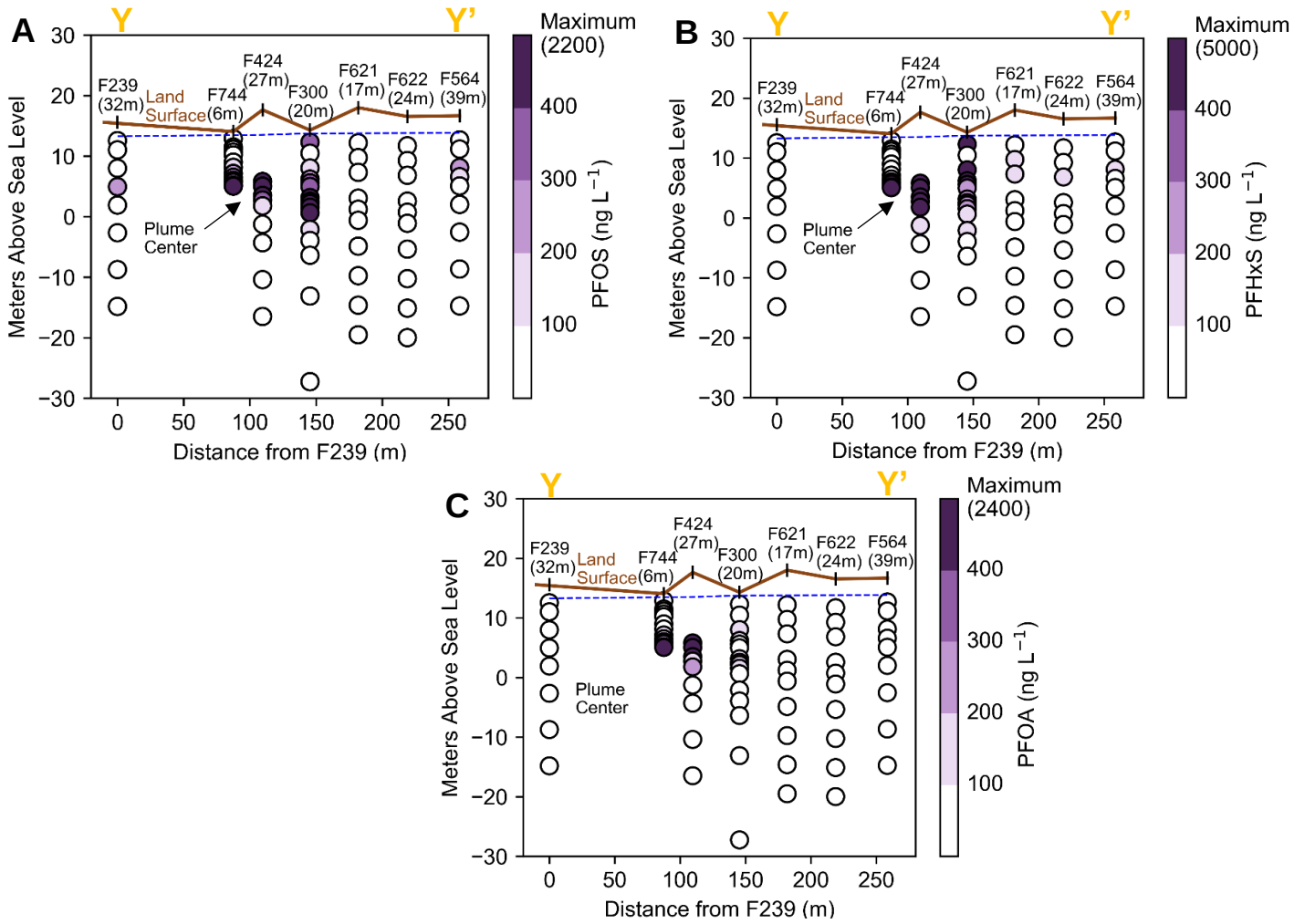

Fig. S2 (A) perfluorooctane sulfonate (PFOS), (B) perfluorohexane sulfonate **(**PFHxS), and (C) perfluorooctanoate (PFOA) concentrations in the transect of wells located upgradient from Ashumet Pond along the Y-Y' transect (Fig. 1B). Flow direction can be visualized as coming out of the page (perpendicular to the cross section). Sea level is referenced to the National Geodetic Vertical Datum of 1929 (NGVD 29). The blue dashed line indicates the water-table altitude. The distance (m) from the shoreline of Ashumet Pond is provided below each well label.

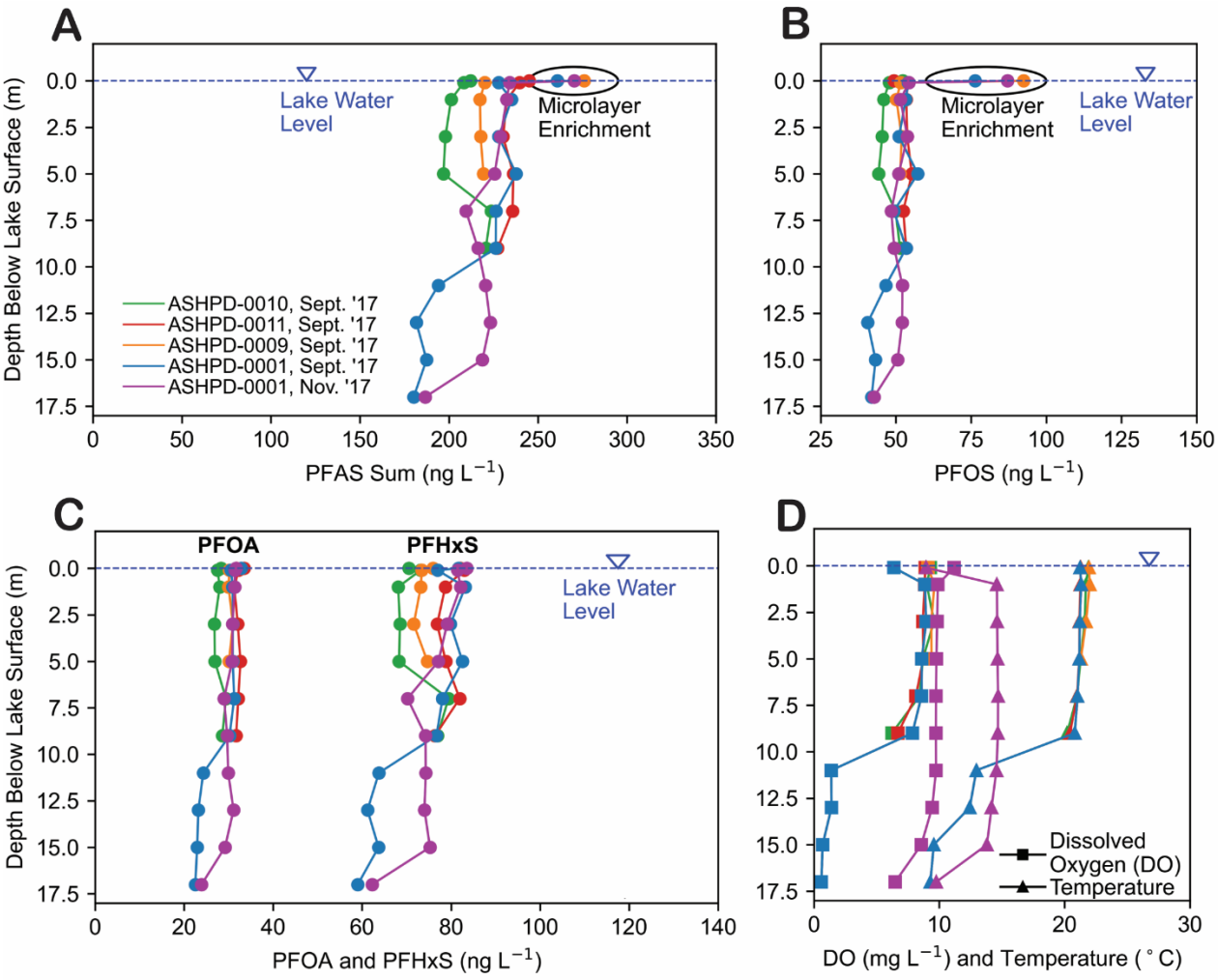

Fig. S3 Profiles in Ashumet Pond showing (A) the sum of quantified per- and polyfluoroalkyl substances (PFAS), (B) perfluorooctane sulfonate (PFOS), (C) perfluorooctanoate (PFOA) and perfluorohexane sulfonate **(**PFHxS), and (D) dissolved oxygen (DO) (squares) and temperature (triangles). Colors shown in the legend in (A) represent sample location and date and apply to plots A through D. Green lines represent ASHPD-0010 in September 2017, red lines represent ASHPD-0011 in September 2017, orange lines represent ASHPD-0009 in September 2017, blue lines represent ASHPD-0001 in September 2017, and purple lines represent ASHPD-0001 in November 2017. See additional Ashumet Pond concentration data from February 2018 and February 2019 in Figure 4 and Figures S5 – S10.

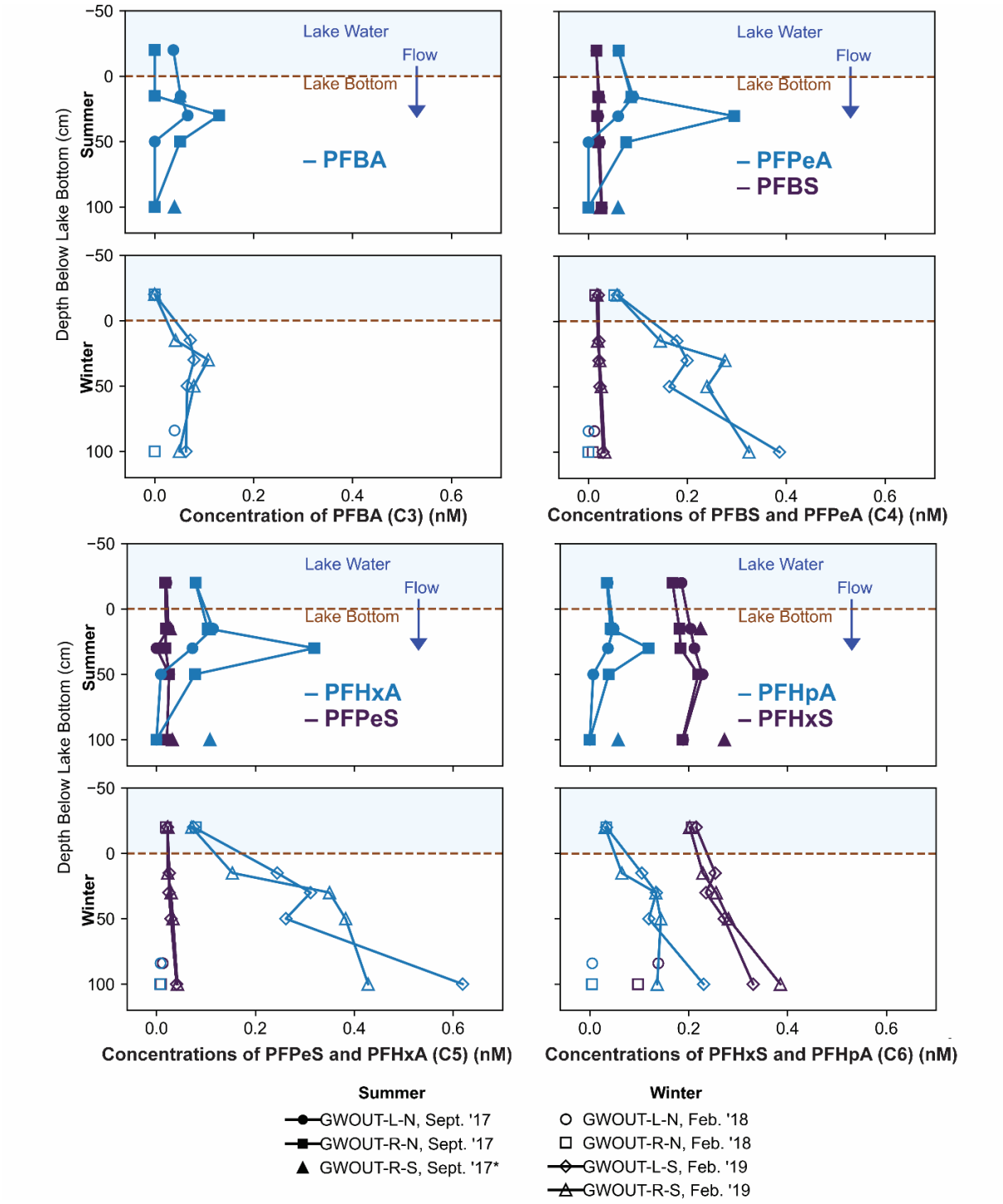

Fig. S4A Seasonal fluctuations in perfluoroalkyl acids (PFAA) at the surface-water/groundwater boundary. Vertical depth profiles for perfluoroalkyl carboxylates (PFCA) and perfluoroalkyl sulfonates (PFSA) at downwelling sites in September 2017, February 2018, and February 2019. Concentrations below the method quantification limit (MQL) are plotted as zero for visual reference. *Site GWOUT-R-S sampled in September 2017 was landward of the lake shore due to low water level in Ashumet Pond; the samples are from 15 and 100 cm below the water table, located 40 cm below the ground surface.

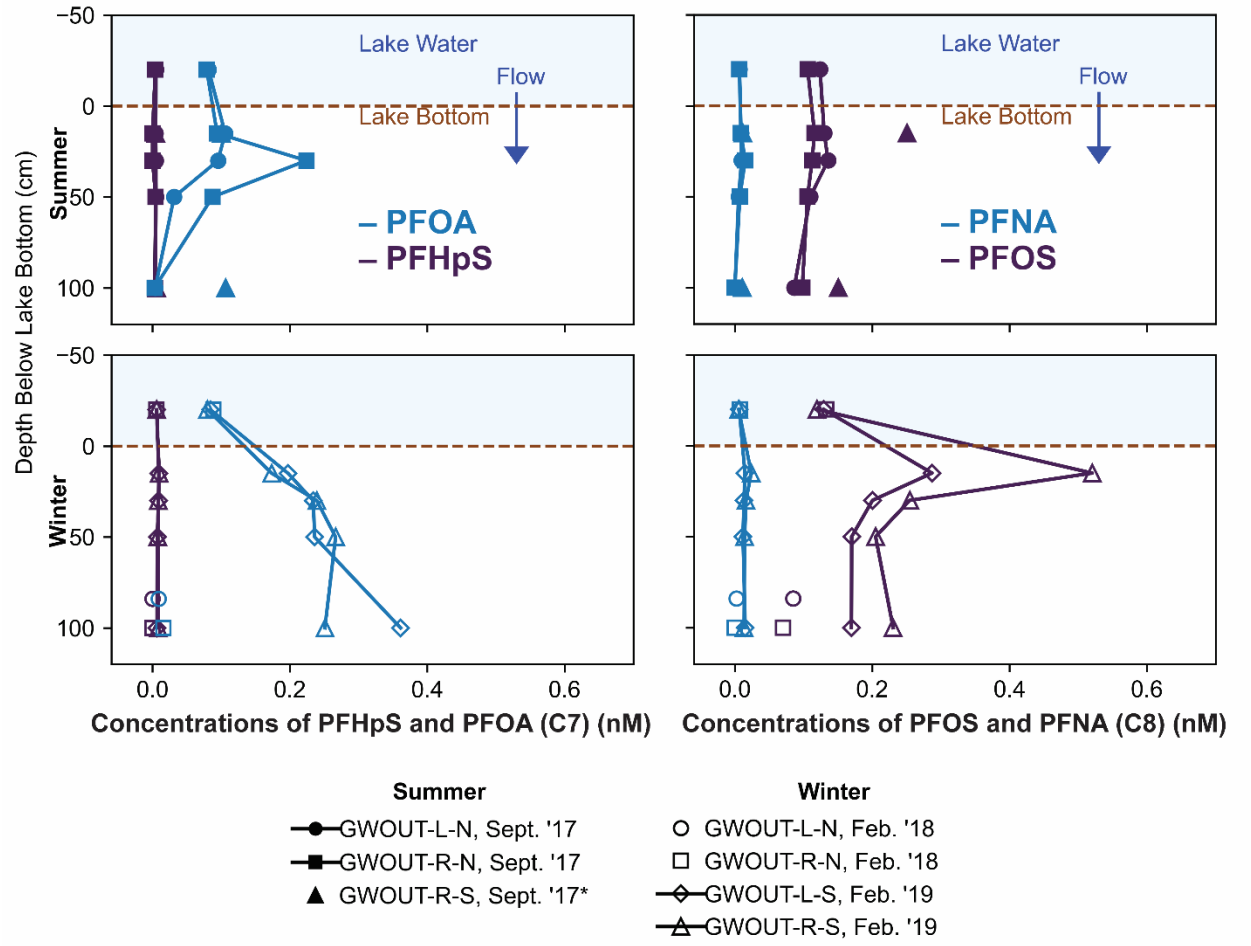

Fig. S4B Seasonal fluctuations in perfluoroalkyl acids (PFAA) at the surface-water/groundwater boundary. Vertical depth profiles for perfluoroalkyl carboxylates (PFCA) and perfluoroalkyl sulfonates (PFSA) at downwelling sites in September 2017, February 2018, and February 2019. Concentrations below the method quantification limit (MQL) are plotted as zero for visual reference. *Site GWOUT-R-S sampled in September 2017 was landward of the lake shore due to low water level in Ashumet Pond; the samples are from 15 and 100 cm below the water table, located 40 cm below the ground surface.

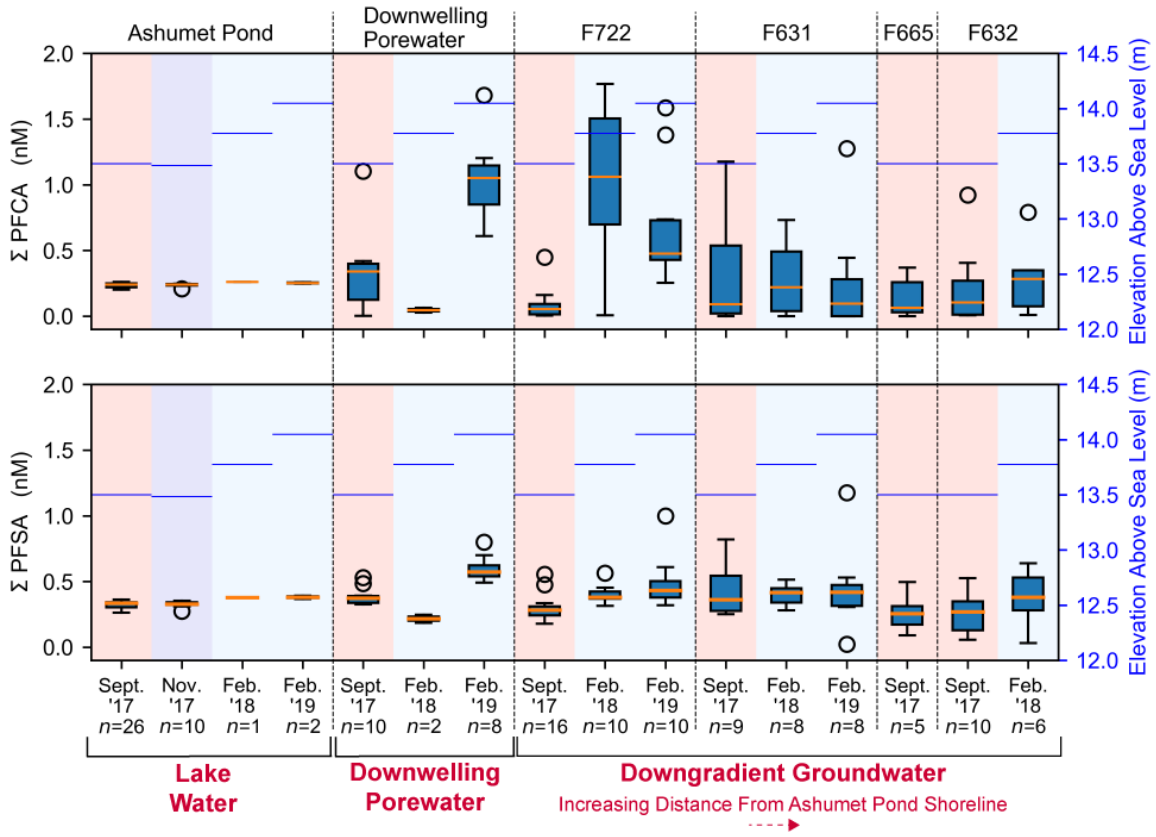

Fig. S5 The sum of measured perfluoroalkyl carboxylates (PFCA) and perfluoroalkyl sulfonates (PFSA) concentrations in nanomolar along the hydrological flow path (from left to right). See Fig. 4 for description of box plot. Lake-water samples from February 2018 and 2019 were collected 20 cm above the lake bottom at the downwelling porewater sampling locations. The lake water surface elevation above mean sea level (National Geodetic Vertical Datum of 1929) in Ashumet Pond[10] associated with each sampling event is shown on the right axis in blue.

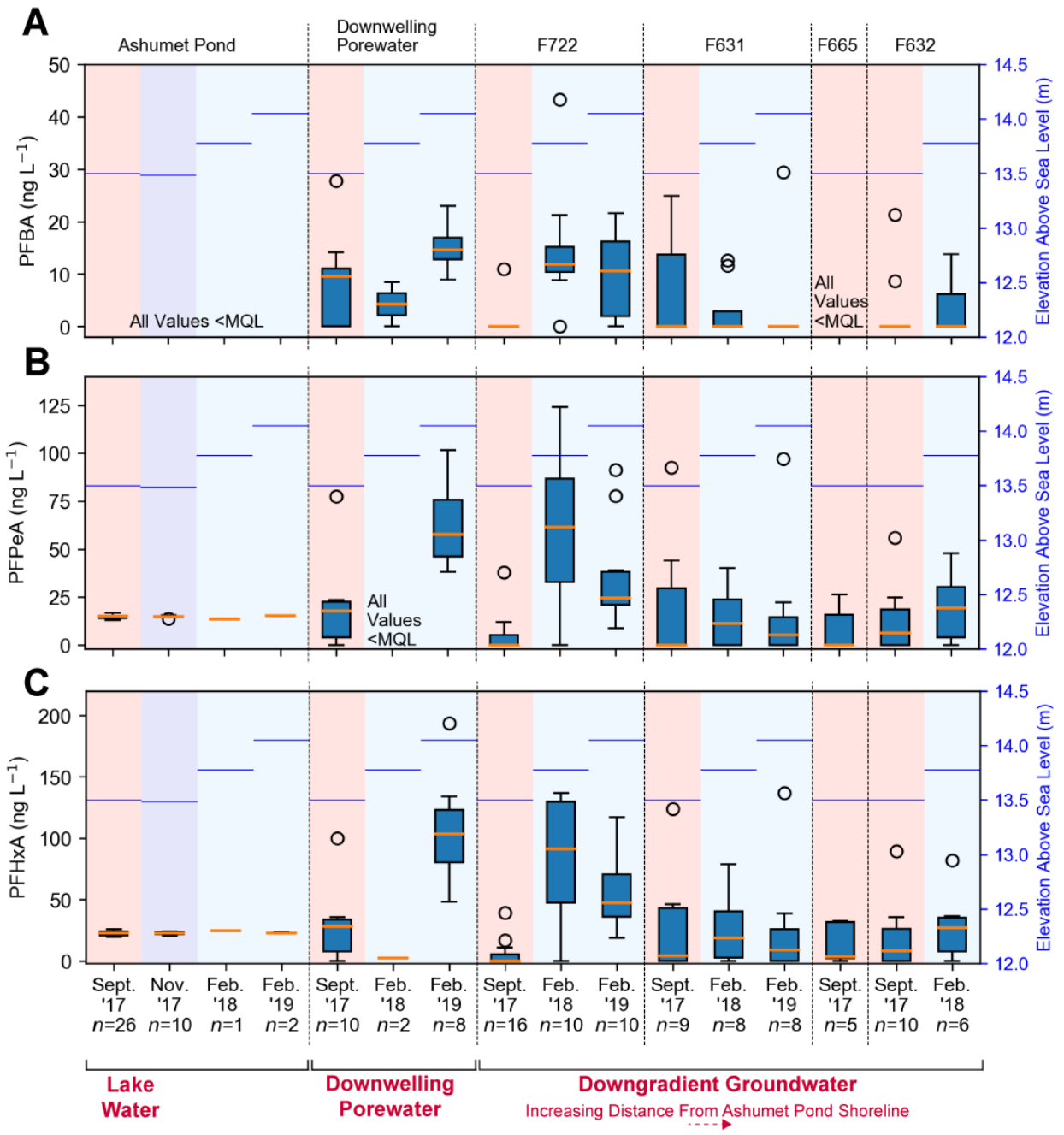

Fig. S6 (A) perfluorobutanoate (PFBA), (B) perfluoropentanoate (PFPeA), and (C) perfluorohexanoate (PFHxA) concentrations along the hydrological flow path (from left to right). See Fig. 4 for description of box plot. Lake-water samples from February 2018 and 2019 were collected 20 cm above the lake bottom at the downwelling porewater sampling locations. The lake water surface elevation above mean sea level (National Geodetic Vertical Datum of 1929) in Ashumet Pond[10] associated with each sampling event is shown on the right axis in blue.

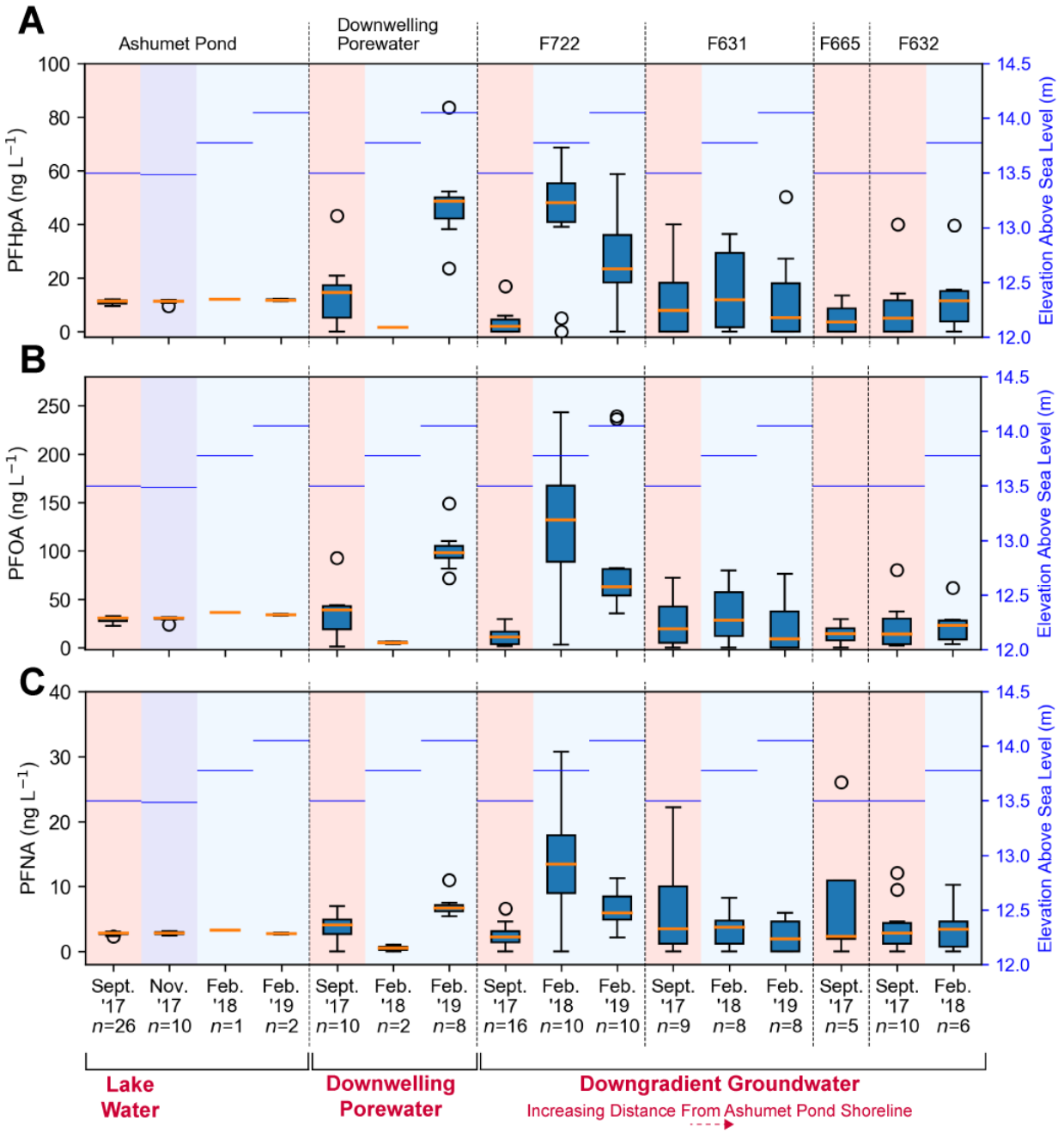

Fig. S7 (A) perfluoroheptanoate (PFHpA), (B) perfluorooctanoate (PFOA), and (C) perfluorononanoate (PFNA) concentrations along the hydrological flow path (from left to right). See Fig. 4 for description of box plot. Lake-water samples from February 2018 and 2019 were collected 20 cm above the lake bottom at the downwelling porewater sampling locations. The lake water surface elevation above mean sea level (National Geodetic Vertical Datum of 1929) in Ashumet Pond[10] associated with each sampling event is shown on the right axis in blue.

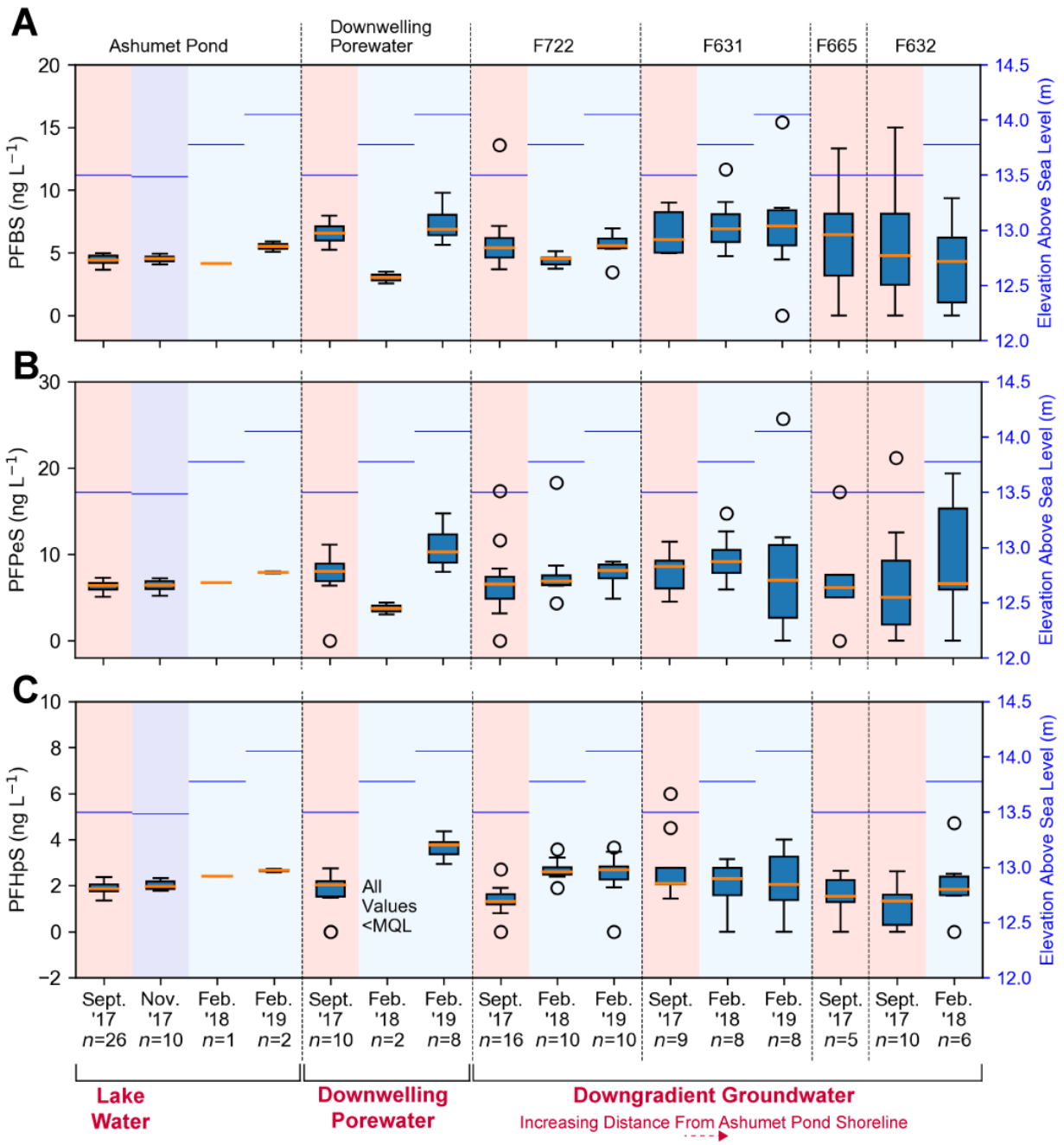

Fig. S8 (A) perfluorobutane sulfonate (PFBS), (B) perfluoropentane sulfonate (PFPeS), and (C) perfluoroheptane sulfonate (PFHpS) concentrations along the hydrological flow path (from left to right). See Fig. 4 for description of box plot. Lake-water samples from February 2018 and 2019 were collected 20 cm above the lake bottom at the downwelling porewater sampling locations. The lake water surface elevation above mean sea level (National Geodetic Vertical Datum of 1929) in Ashumet Pond[10] associated with each sampling event is shown on the right axis in blue.

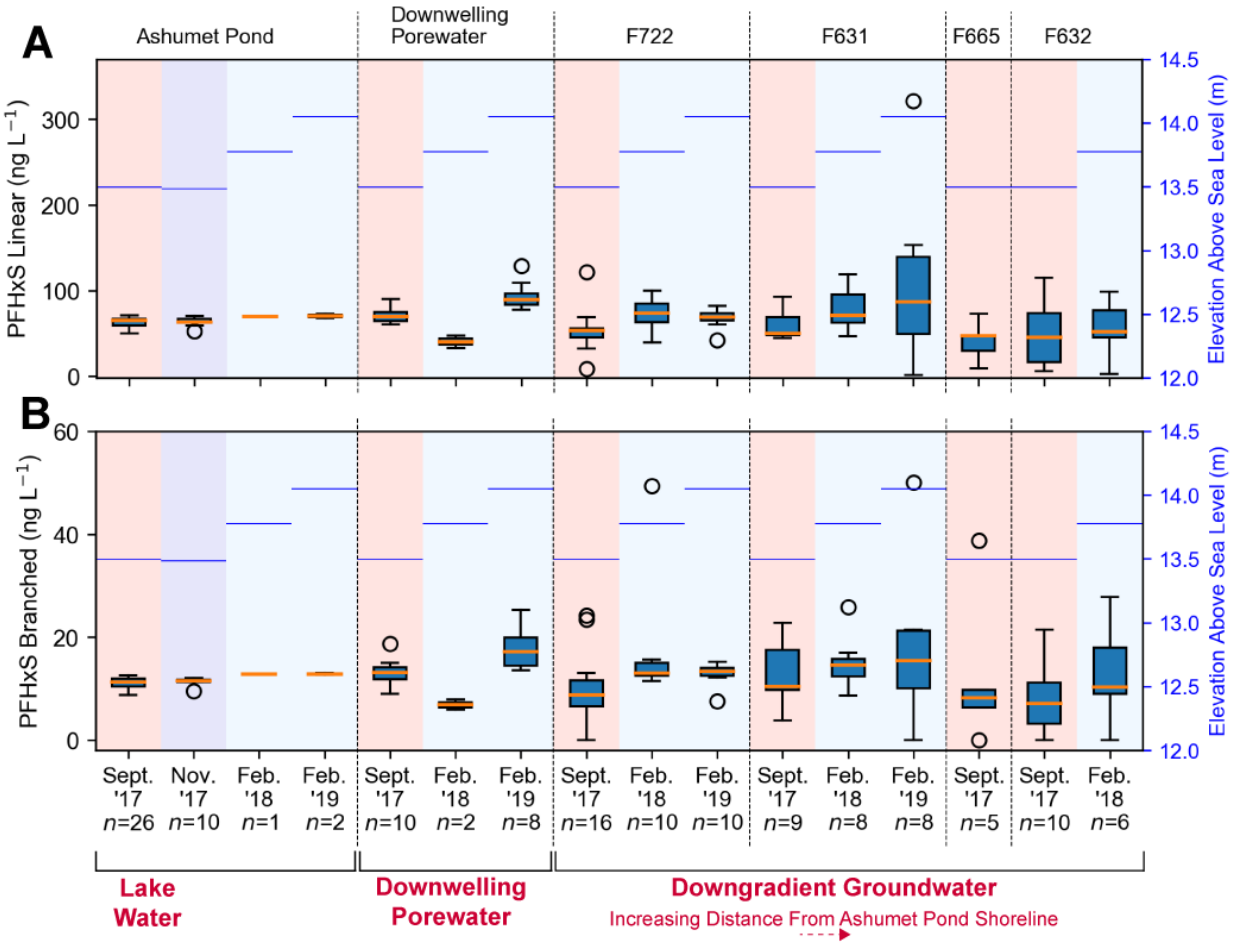

Fig. S9 (A) Linear perfluorohexane sulfonate (PFHxS) and (B) Branched PFHxS concentrations along the hydrological flow path (from left to right). See Fig. 4 for description of box plot. Lake-water samples from February 2018 and 2019 were collected 20 cm above the lake bottom at the downwelling porewater sampling locations. The lake water surface elevation above mean sea level (National Geodetic Vertical Datum of 1929) in Ashumet Pond[10] associated with each sampling event is shown on the right axis in blue.

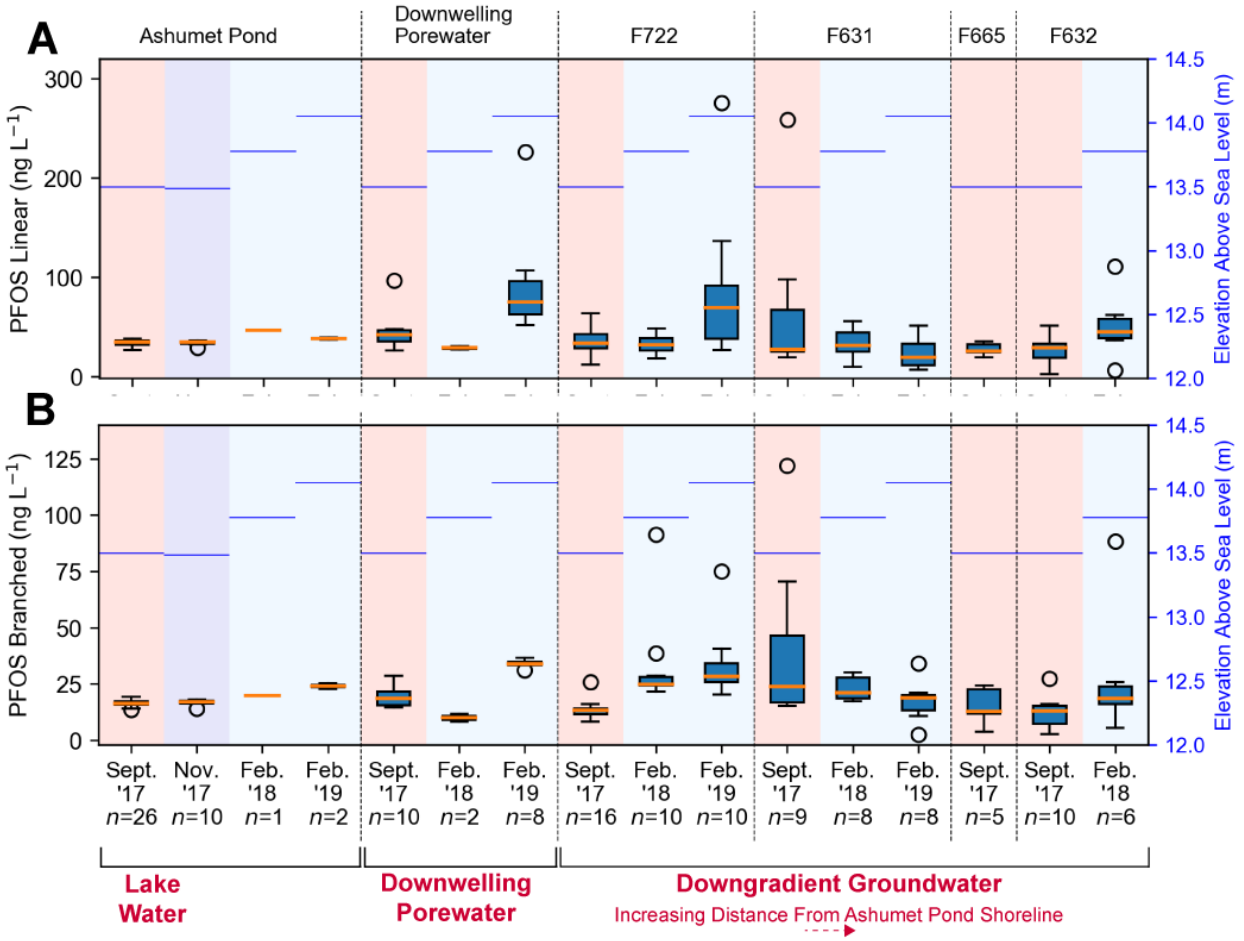

Fig. S10 (A) Linear perfluorooctane sulfonate (PFOS) and (B) Branched PFOS concentrations along the hydrological flow path (from left to right). See Fig. 4 for description of box plot. Lake-water samples from February 2018 and 2019 were collected 20 cm above the lake bottom at the downwelling porewater sampling locations. The lake water surface elevation above mean sea level (National Geodetic Vertical Datum of 1929) in Ashumet Pond[10] associated with each sampling event is shown on the right axis in blue.

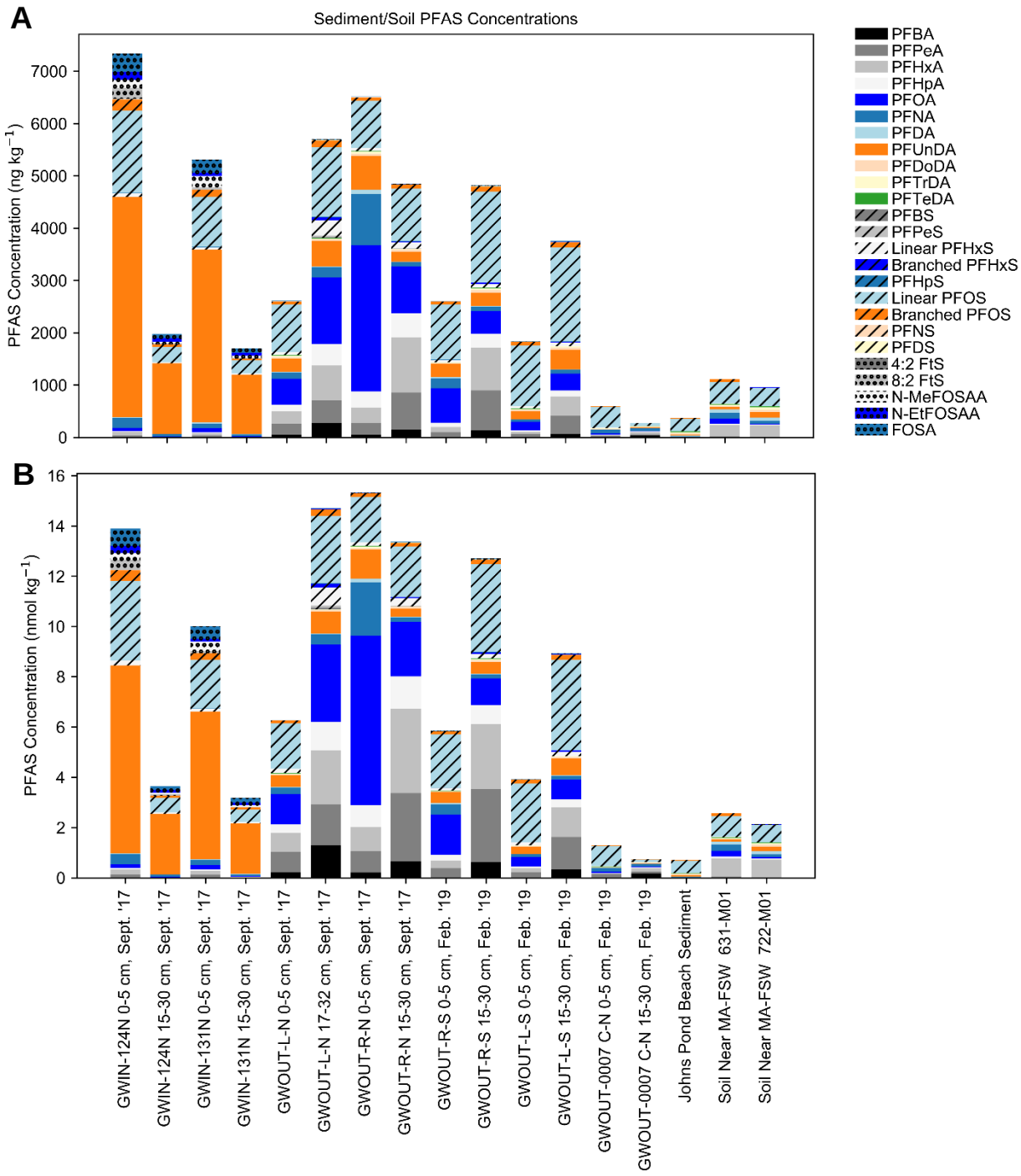

Fig. S11 Per- and polyfluoroalkyl substances (PFAS) concentrations in (A) ng kg^{-1} and (B) nmol kg^{-1} in sediment and soil samples in and around Ashumet Pond and Johns Pond.

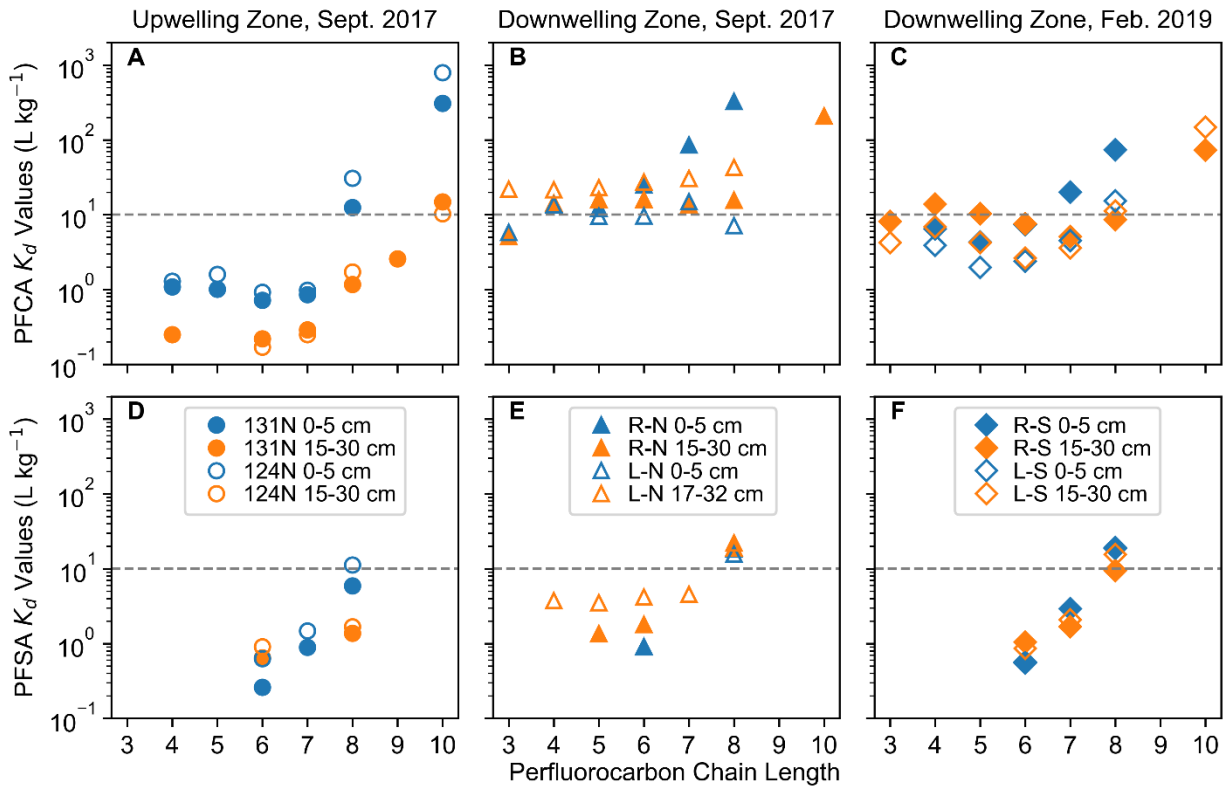

Fig. S12 Sediment/water distribution coefficient (K_d) values by perfluorocarbon chain length for upwelling porewater in September 2017 (circles), downwelling porewater in September 2017 (triangles), and downwelling porewater in February 2019 (diamonds) in Ashumet Pond. The dashed grey line is a visual aid to compare the top and bottom rows. The sampled intervals are depth relative to the lake bottom.

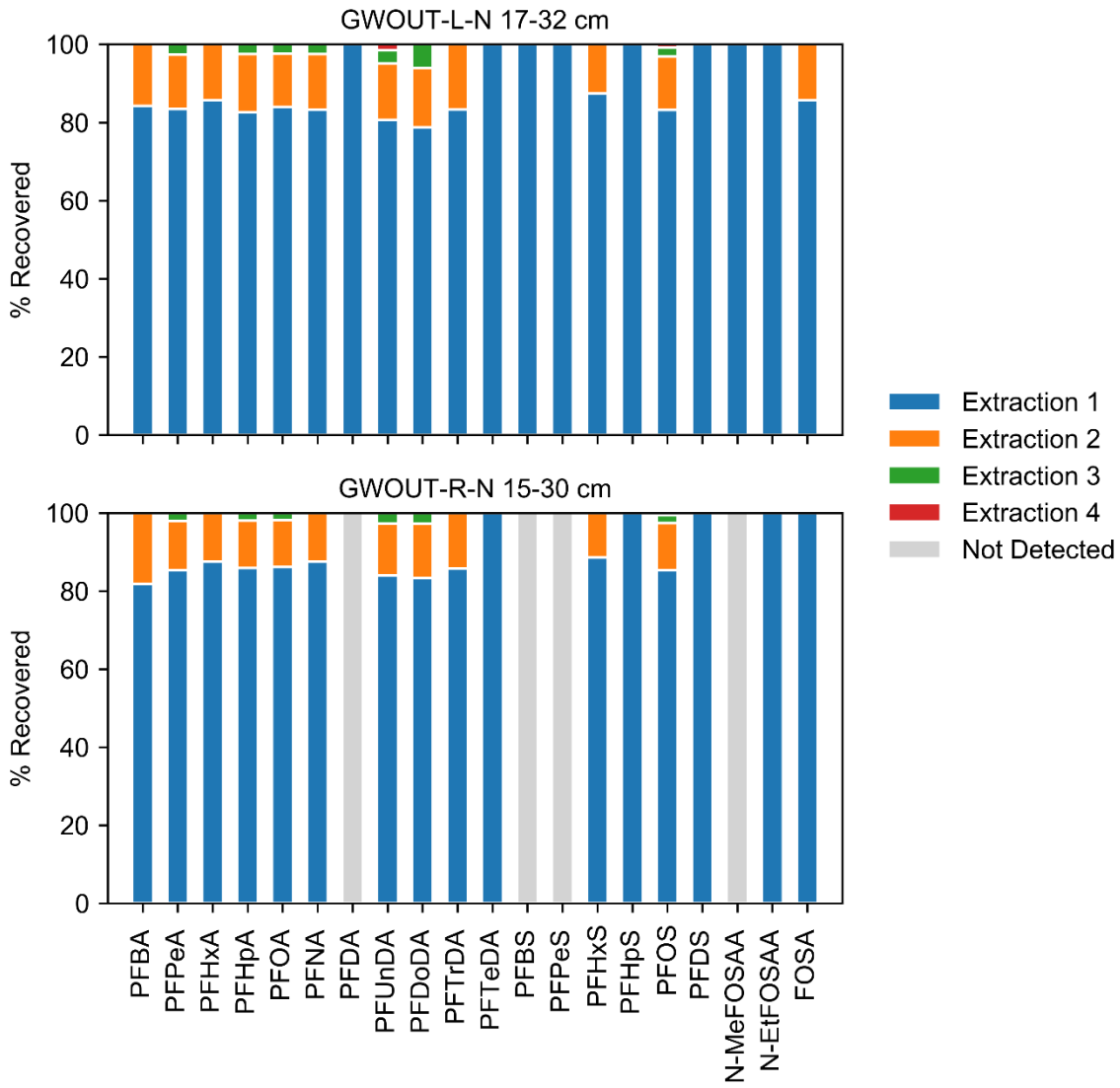

Fig. S13 The fraction of per- and polyfluoroalkyl substances (PFAS) recovered for four sequential extractions conducted on two sediment samples from Ashumet Pond.

Any use of trade, firm, or product names is for descriptive purposes only and does not imply endorsement by the U.S. Government.

References

1. S. P. Garabedian, D. R. LeBlanc, L. W. Gelhar and M. A. Celia, Large-scale natural gradient tracer test in sand and gravel, Cape Cod, Massachusetts: 2. Analysis of spatial moments for a nonreactive tracer, *Water Resour. Res.*, 1991, **27**, 911-924.
2. D. R. LeBlanc, S. P. Garabedian, K. M. Hess, L. W. Gelhar, R. D. Quadri, K. G. Stollenwerk and W. W. Wood, Large-scale natural gradient tracer test in sand and gravel, Cape Cod, Massachusetts: 1. Experimental design and observed tracer movement, *Water Resour. Res.*, 1991, **27**, 895-910.
3. D. A. Walter, T. D. McCobb, J. P. Masterson and M. N. Fienen, *Potential effects of sea-level rise on the depth to saturated sediments of the Sagamore and Monomoy flow lenses on Cape Cod, Massachusetts*, U.S. Geological Survey Scientific Investigations Report 2016-5058; U.S. Geological Survey: Reston, VA, 2016.
4. D. R. LeBlanc, *Sewage plume in a sand and gravel aquifer, Cape Cod, Massachusetts*, U.S. Geological Survey Water-Supply Paper 2218; U.S. Geological Survey: Reston, VA, 1984.
5. T. D. McCobb, D. R. LeBlanc, D. A. Walter, K. M. Hess, D. B. Kent and R. L. Smith, *Phosphorus in a ground-water contaminant plume discharging to Ashumet Pond, Cape Cod, Massachusetts, 1999*, U.S. Geological Survey Water-Resources Investigations Report 02-4306; U. S. Geological Survey: Reston, VA, 2003.
6. D. A. Walter and J. P. Masterson, *Estimated hydrologic budgets of kettle-hole ponds in coastal aquifers of southeastern Massachusetts*, U.S. Geological Survey Scientific Investigations Report 2011-5137; U.S. Geological Survey: Reston, VA, 2011.
7. D. L. Stoliker, D. A. Repert, R. L. Smith, B. Song, D. R. LeBlanc, T. D. McCobb, C. H. Conaway, S. P. Hyun, D.-C. Koh, H. S. Moon and D. B. Kent, Hydrologic controls on nitrogen cycling processes and functional gene abundance in sediments of a groundwater flow-through lake, *Environ. Sci. Technol.*, 2016, **50**, 3649-3657.
8. R. L. Smith, D. A. Repert, D. L. Stoliker, D. B. Kent, B. Song, D. R. LeBlanc, T. D. McCobb, J. K. Böhlke, S. P. Hyun and H. S. Moon, Seasonal and spatial variation in the location and reactivity of a nitrate-contaminated groundwater discharge zone in a lakebed, *J. Geophys. Res.: Biogeosciences*, 2019, **124**, 2186-2207.
9. R. B. Hull, M. A. Briggs, D. R. LeBlanc, D. A. Armstrong and T. D. McCobb, *Temperature and seepage data from the nearshore bottom sediments of five groundwater flow-through glacial kettle lakes, western Cape Cod, Massachusetts, 2015-18*, U.S. Geological Survey data release; U.S. Geological Survey: Reston, VA, 2019.
10. National Water Information System, National Water Information System: Mapper, https://maps.waterdata.usgs.gov/mapper/index.html, (accessed May 12, 2020, 2020).
11. J. G. Savoie, D. R. LeBlanc, G. M. Fairchild, R. L. Smith, D. B. Kent, L. B. Barber, D. A. Repert, C. P. Hart, S. H. Keefe and L. A. Parsons, *Groundwater-quality data for a treated-wastewater plume near the Massachusetts Military Reservation, Ashumet Valley, Cape Cod, Massachusetts, 2006–08*, U.S. Geological Survey Data Series 648; U.S. Geological Survey: Reston, VA, 2012.
12. A. K. Weber, L. B. Barber, D. R. LeBlanc, E. M. Sunderland and C. D. Vecitis, Geochemical and hydrologic factors controlling subsurface transport of poly- and perfluoroalkyl substances, Cape Cod, Massachusetts, *Environ. Sci. Technol.*, 2017, **51**, 4269-4279.

13. X. Ju, Y. Jin, K. Sasaki and N. Saito, Perfluorinated surfactants in surface, subsurface water and microlayer from Dalian coastal waters in China, *Environ. Sci. Technol.*, 2008, **42**, 3538-3542.
14. A. K. Tokranov, H. M. Pickard, D. R. LeBlanc, B. J. Ruyle, R. B. Hull, L. B. Barber, D. A. Repert, E. M. Sunderland and C. D. Vecitis, *Concentrations of per- and polyfluoroalkyl substances (PFAS) and related chemical and physical data at and near surface-water/groundwater boundaries on Cape Cod, Massachusetts, 2016-19*, U.S. Geological Survey data release; U.S. Geological Survey: Reston, VA, 2021, https://doi.org/10.5066/P9HPBFRT.
15. E. F. Houtz, C. P. Higgins, J. A. Field and D. L. Sedlak, Persistence of perfluoroalkyl acid precursors in AFFF-impacted groundwater and soil, *Environ. Sci. Technol.*, 2013, **47**, 8187-8195.
16. E. F. Houtz and D. L. Sedlak, Oxidative conversion as a means of detecting precursors to perfluoroalkyl acids in urban runoff, *Environ. Sci. Technol.*, 2012, **46**, 9342-9349.
17. B. J. Ruyle, H. M. Pickard, D. R. LeBlanc, A. K. Tokranov, C. P. Thackray, X. C. Hu, C. D. Vecitis and E. M. Sunderland, Isolating the AFFF Signature in Coastal Watersheds Using Oxidizable PFAS Precursors and Unexplained Organofluorine, *Environ. Sci. Technol.*, 2021, **55**, 3686-3695.
18. B. J. Ruyle, C. P. Thackray, J. P. McCord, M. J. Strynar, K. A. Mauge-Lewis, S. E. Fenton and E. M. Sunderland, Reconstructing the composition of per- and polyfluoroalkyl substances in contemporary aqueous film-forming foams, *Environ. Sci. Technol. Lett.*, 2021, **8**, 59-65.
19. D. Foreman-Mackey, D. W. Hogg, D. Lang and J. Goodman, emcee: The MCMC hammer, *Publications of the Astronomical Society of the Pacific*, 2013, **125**, 306-312.
20. B. Nelson, E. B. Ford and M. J. Payne, RUN DMC: An efficient, parallel code for Analyzing radial velocity observations using n-Body integrations and differential evolution Markov Chain Monte Carlo, *The Astrophysical Journal Supplement Series*, 2013, **210**, 11.
21. M. E. Tuccillo, I. M. Cozzarelli and J. S. Herman, Iron reduction in the sediments of a hydrocarbon-contaminated aquifer, *Appl. Geochem.*, 1999, **14**, 655-667.
22. H. Agemian and A. S. Y. Chau, A study of different analytical extraction methods for nondetrital heavy metals in aquatic sediments, *Arch. Environ. Contamin. and Toxicol.*, 1977, **6**, 69-82.
23. Z. Wang, J. C. DeWitt, C. P. Higgins and I. T. Cousins, A never-ending story of per- and polyfluoroalkyl substances (PFASs)?, *Environ. Sci. Technol.*, 2017, **51**, 2508-2518.
24. T. Y. Campbell, C. D. Vecitis, B. T. Mader and M. R. Hoffmann, Perfluorinated surfactant chain-length effects on sonochemical kinetics, *J. Phys.Chem. A*, 2009, **113**, 9834-9842.
25. C. D. Vecitis, H. Park, J. Cheng, B. T. Mader and M. R. Hoffmann, Enhancement of perfluorooctanoate and perfluorooctanesulfonate activity at acoustic cavitation bubble interfaces, *J. Phys. Chem. C*, 2008, **112**, 16850-16857.
26. R. W. Harvey, D. W. Metge, D. R. LeBlanc, J. C. Underwood, G. R. Aiken, K. D. Butler, T. D. McCobb and J. Jasperse, Importance of the colmation layer in the transport and removal of cyanobacteria, viruses, and dissolved organic carbon during natural lake-bank filtration, *J. Environ. Qual.*, 2015, **44**, 1413-1423.